



## OPEN ACCESS

## EDITED BY

Dragan Marinkovic,  
Technical University of Berlin, Germany

## REVIEWED BY

S. A. Edalatpanah,  
Ayandegan Institute of Higher Education  
(AIHE), Iran  
Arzu Akbulut,  
Bursa Uludağ University, Türkiye  
Shah Muhammad,  
King Saud University, Saudi Arabia  
Ain Qura Tul,  
Guizhou University, China

## \*CORRESPONDENCE

Anam Nigar,  
✉ nigaranam@yahoo.com

RECEIVED 01 June 2023

ACCEPTED 17 August 2023

PUBLISHED 17 October 2023

## CITATION

Ali A, Nigar A, Nadeem M, Jat Baloch MY,  
Farooq A, Alrefaei AF and Hussain R  
(2023), Complex solutions for nonlinear  
fractional partial differential equations via  
the fractional conformable residual  
power series technique and modified  
auxiliary equation method.  
*Front. Phys.* 11:1232828.  
doi: 10.3389/fphy.2023.1232828

## COPYRIGHT

© 2023 Ali, Nigar, Nadeem, Jat Baloch,  
Farooq, Alrefaei and Hussain. This is an  
open-access article distributed under the  
terms of the [Creative Commons  
Attribution License \(CC BY\)](https://creativecommons.org/licenses/by/4.0/). The use,  
distribution or reproduction in other  
forums is permitted, provided the original  
author(s) and the copyright owner(s) are  
credited and that the original publication  
in this journal is cited, in accordance with  
accepted academic practice. No use,  
distribution or reproduction is permitted  
which does not comply with these terms.

# Complex solutions for nonlinear fractional partial differential equations via the fractional conformable residual power series technique and modified auxiliary equation method

Asgar Ali<sup>1</sup>, Anam Nigar<sup>2\*</sup>, Muhammad Nadeem<sup>3</sup>,  
Muhammad Yousuf Jat Baloch<sup>4</sup>, Atiya Farooq<sup>5</sup>,  
Abdulwahed Fahad Alrefaei<sup>6</sup> and Rashida Hussain<sup>5</sup>

<sup>1</sup>Mirpur University of Science and Technology (MUST), Mirpur, Pakistan, <sup>2</sup>School of Electronics and Information Engineering, Changchun University of Science and Technology, Changchun, China, <sup>3</sup>School of Mathematics and Statistics, Qijing Normal University, Qijing, China, <sup>4</sup>College of New Energy and Environment, Jilin University, Changchun, China, <sup>5</sup>Department of Mathematics, Mirpur University of Science and Technology, Mirpur, Pakistan, <sup>6</sup>Department of Zoology, College of Science, King Saud University, Riyadh, Saudi Arabia

The fractional-order nonlinear Gardner and Cahn–Hilliard equations are often used to model ultra-short burst beams of light, complex fields of optics, photonic transmission systems, ions, and other fields of mathematical physics and engineering. This study has two main objectives. First, the main objective of this investigation is to solve the fractional-order nonlinear Gardner and Cahn–Hilliard equations by using the modified auxiliary equation method, which is not found in the literature. Second, the exact and approximate solutions of these equations are obtained by utilizing the fractional conformable residual power series algorithm and the modified auxiliary equation method. For the analytical and numerical solutions to two equations, we employ two separate techniques and establish consistency between the precise answers that are derived and the compatible numerical solution. To the best of our knowledge, this method of solving equations has never been investigated in this manner. The 2D and 3D contours have been defined using appropriate parametric values to support the physical compatibility of the results. The assessed findings suggested that the approach used in this study to recover inclusive and standard solutions is approachable, efficient, and faster in computing and can be considered a useful tool in resolving more complex phenomena that arise in the field of engineering, mathematical physics, and optical fiber.

## KEYWORDS

fractional conformable residual power series algorithm, nonlinear partial differential equations, fractional-order nonlinear Cahn–Hilliard equation, modified auxiliary equation method, approximate solution

# 1 Introduction

In complicated areas of fields that can be modeled by various types of partial differential equations, many linear and nonlinear solutions appear. The nonlinear partial differential equations (NLPDEs) are crucial for studying a variety of issues. Understanding virtually nonlinear partial differential equations requires an effort to determine precise solutions to nonlinear equations [1–3]. Fractional calculus, which is the study of integrals and derivatives of any arbitrary real or complex order, has gained significant recognition over the past 30 years or so largely because of its well-established applications in numerous and varied disciplines of technical knowledge [4].

Fractional differential equations have received considerable attention over the past 20 years as a result of their capacity to accurately reproduce a broad range of events in a variety of

scientific and technical fields. In science and engineering, fractional differential equations can be used to represent a variety of physical applications [5]. Fractional differential equations have been used to tackle numerous engineering and scientific problems [6]. The differential equation in fractional nonlinear partial differential equations (FNLNLPDEs) has nonlinear variables which create complex behaviors and phenomena not seen in linear equations. Complex patterns, chaotic dynamics, solitons, and shocks can all occur as a result of nonlinearity. The interaction between nonlinearity and fractional derivatives makes it particularly difficult to comprehend and analyze the dynamics of FNLNLPDEs.

The usage of fractional differential equations (FDEs) is widespread throughout many scientific disciplines due to their various applications in physics and engineering. Fractional partial differential equations (FPDEs) have grown in

**TABLE 1 Comparison of analytical solutions via the MSSE technique and numerical solutions computed via the modified VI technique for the model under investigation.**

Iteration	Analytical	Numerical	Absolute error	Relative error
1	6.2	23	17	2.8333
2	2.2	11	9	4.5
3	-19.2	-22	3	0.15789
4	-75.2	-94	19	0.25333
5	-190.2	-229	39	0.20526
6	-394.2	-457	63	0.1599
7	-723.2	-814	91	0.12586
8	-1219.2	-1342	123	0.1009
9	-1930.2	-2089	159	0.082383
21	-52894.2	-53797	903	0.017072
22	-63498.2	-64489	991	0.015607
23	-75619.2	-76702	1083	0.014322
24	-89395.2	-90574	1179	0.013189
25	-1.0497e + 05	-1.0625e + 05	1279	0.012184
26	-1.2249e + 05	-1.2388e + 05	1383	0.01129
27	-1.4212e + 05	-1.4361e + 05	1491	0.010491
28	-1.6402e + 05	-1.6562e + 05	1603	0.0097733
29	-1.8835e + 05	-1.9007e + 05	1719	0.0091266
30	-2.1529e + 05	-2.1713e + 05	1839	0.008542
31	-2.4502e + 05	-2.4698e + 05	1963	0.0080116
32	-2.7772e + 05	-2.7981e + 05	2091	0.0075291
33	-3.1359e + 05	-3.1582e + 05	2,223	0.0070888
34	-3.5283e + 05	-3.5519e + 05	2,359	0.0066859
35	-3.9564e + 05	-3.9813e + 05	2,499	0.0063164
36	-4.4222e + 05	-4.4486e + 05	2,643	0.0059767
37	-4.928e + 05	-4.9559e + 05	2,791	0.0056636

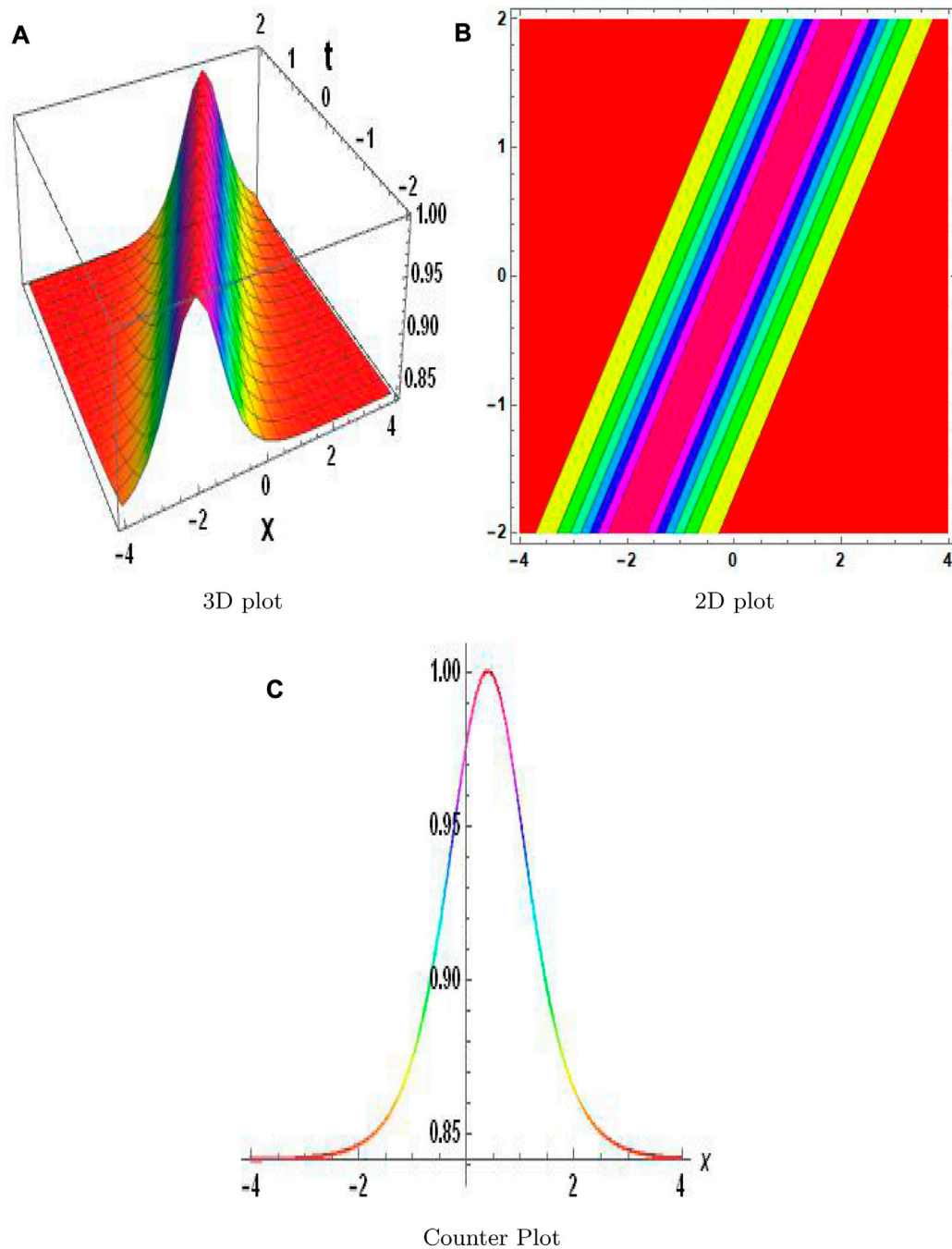
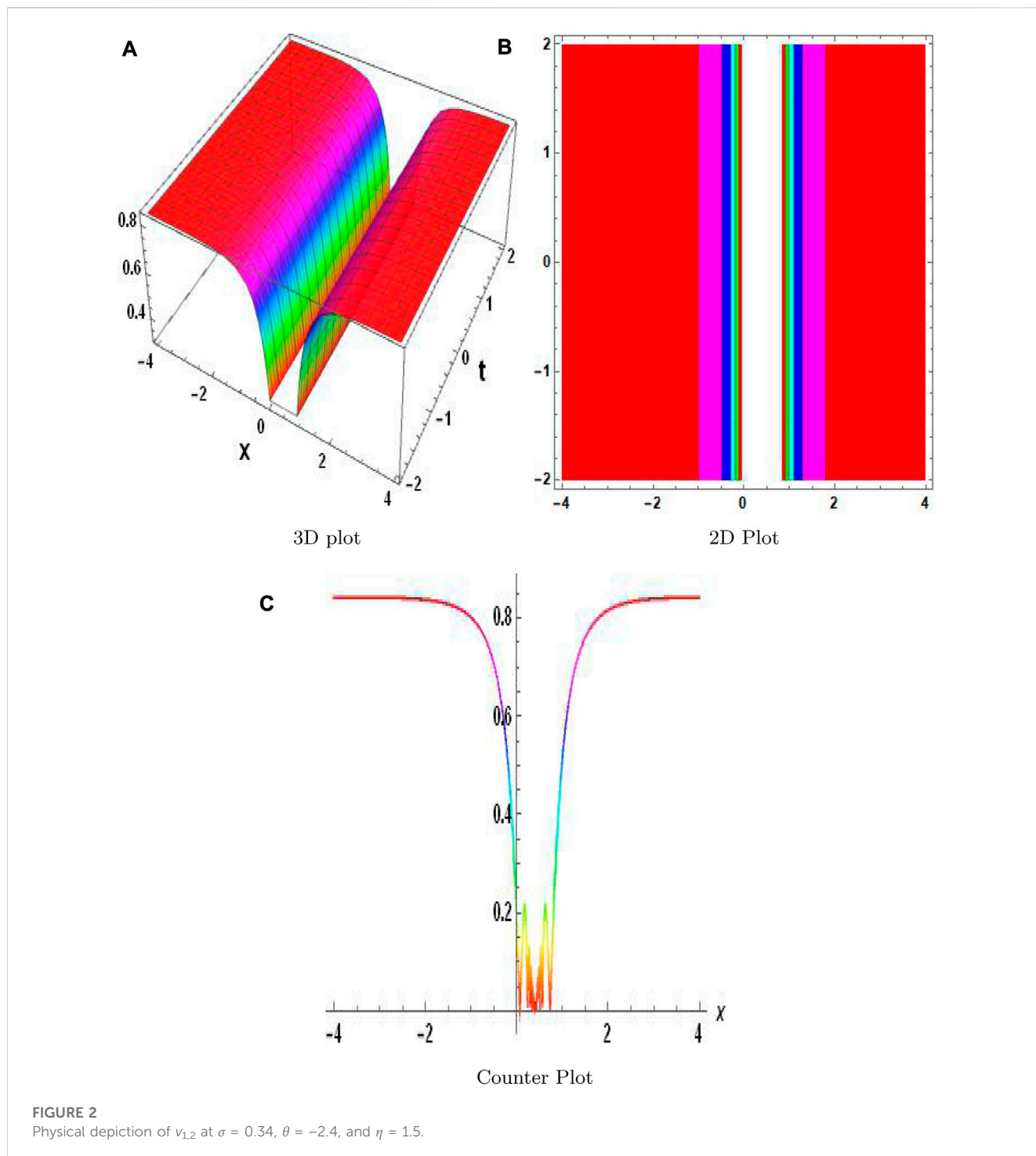


**FIGURE 1**  
Physical depiction of  $v_{1,1}$  at  $\sigma = 0.4$ ,  $\theta = -1.4$ , and  $\eta = 0.5$ .

significance and reputation among FDEs in recent years as a result of their demonstrated utility in a wide range of extremely diverse scientific and engineering disciplines [7]. Many fractional types of equations are solved using novel transform [8] and zz transform with the Mittag-Leffler kernel [9]. Since they cannot be solved precisely, the majority of nonlinear FDEs require approximate and numerical solutions such as the Adomian decomposition method [10], spectral collocation method [11], Euler method and homotopy analysis method [12], Laplace

residual power series [13], variational iteration transform method [14], and homotopy analysis method [15]. FNL PDEs find applications in various cutting-edge areas of research. For example, in materials science, FNL PDEs are used to model diffusion and transport in heterogeneous media. In finance, they are employed to describe complex price dynamics and risk management. In biology, FNL PDEs are utilized to study the spread of diseases and population dynamics. The unique combination of nonlinearity and fractional derivatives in



FNLNDEs provides a versatile framework for modeling these emerging phenomena.

One of the most recent methods developed in this field is the auxiliary equation method proposed by Khater [16]. Although this approach was employed in numerous research studies [17], a modified auxiliary equation approach (also known as the modified Khater method) was developed to get precise traveling wave solutions. The soliton and other solitary wave solutions of the equations are obtained in this research paper using the modified auxiliary equation approach. It enhances the

auxiliary equation method. This article describes a method that modifies the auxiliary differential equation methodology for solving nonlinear partial differential equations [18]. Over the past 30 years, fresh and state-of-the-art methods for investigating nonlinear differential systems with fractional-order equations have been created, along with new computer methods and symbolic programming. Analytical methodologies, new mathematical theories, and computational systems that enable us to study nonlinear complicated phenomena have triggered this revolution in understanding. Furthermore, the sub-equation

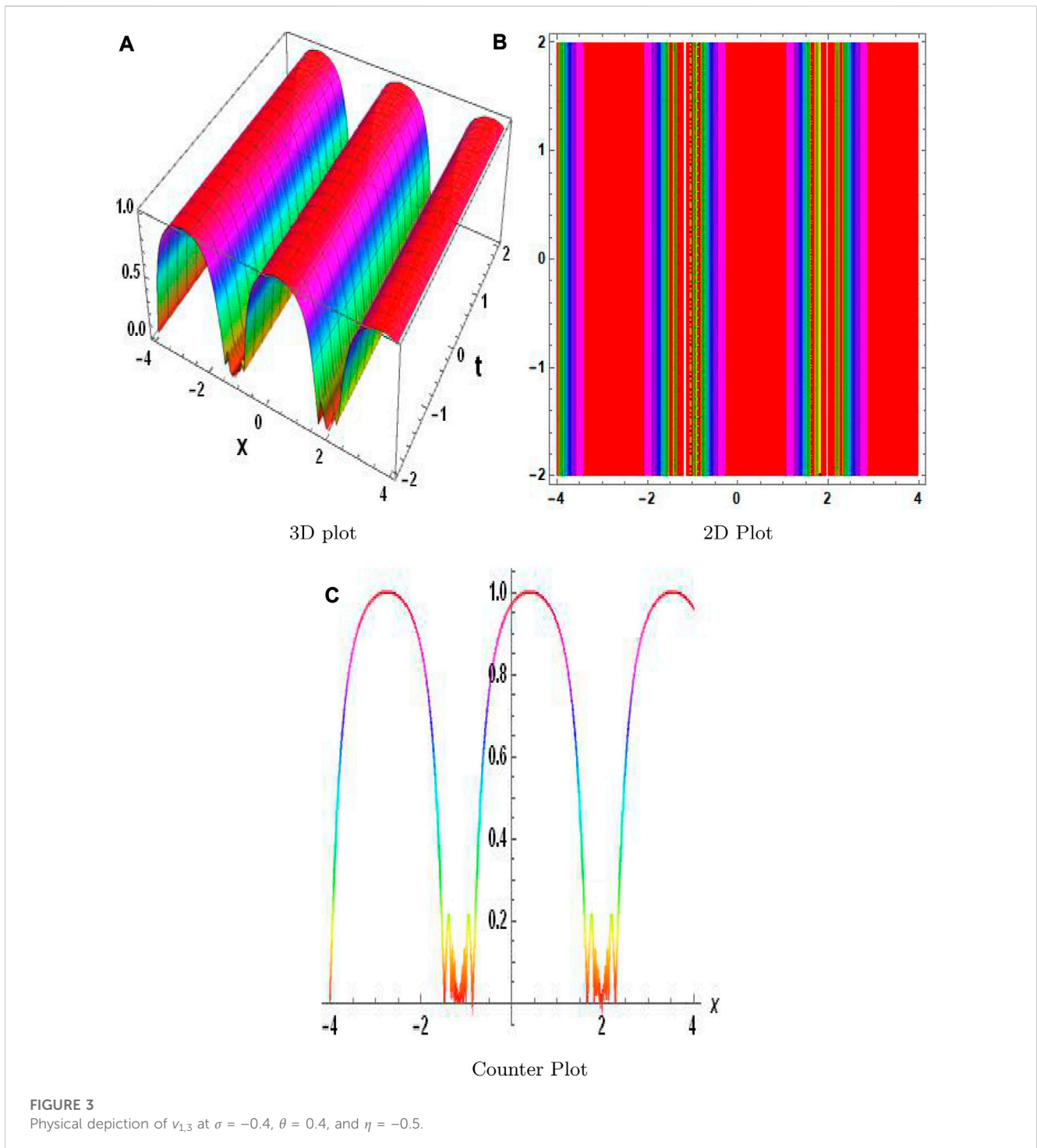


**FIGURE 3**  
Physical depiction of  $v_{1,3}$  at  $\sigma = -0.4$ ,  $\theta = 0.4$ , and  $\eta = -0.5$ .

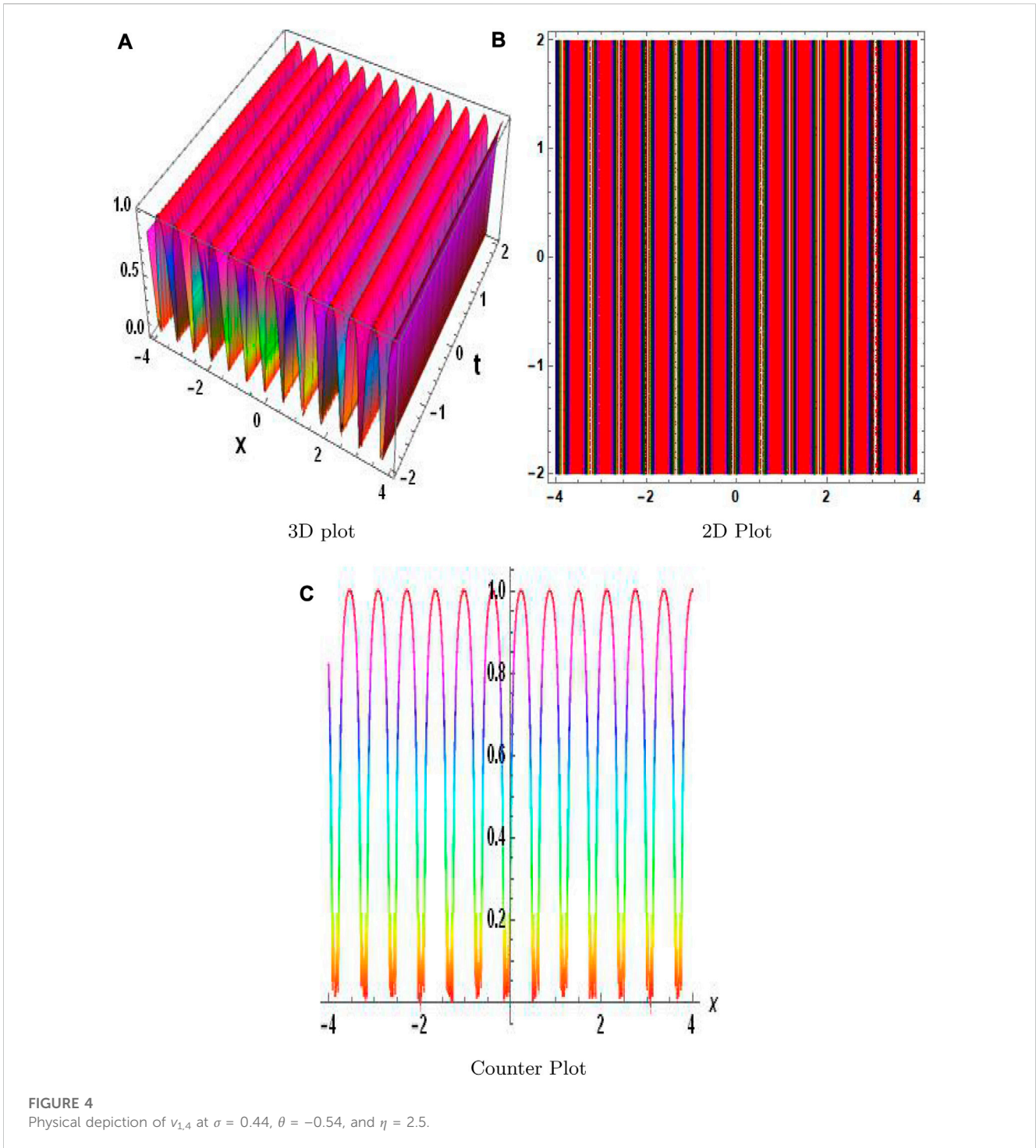
method [19], modified Kudryashov method [20], and F-expansion method [21–23] are just a few of the methods that have been used.

A semi-approximate approach called numerical simulations was developed specifically for addressing challenging nonlinear temporal FPDEs that can appear in a variety of scientific fields. This approach, which was devised and developed by Abu Arqub for the study of fuzzy differential equations, is used for generalizing the expansion of the Taylor series of arbitrary order and minimizing the residual error identified to detect

the unknown compounds. This method has the ability to immediately solve nonlinear terms without any constraints, transformations, linearizations, or changes to the models. As a result, it has attracted considerable attention and has become an energizing focus of the research community [24, 25].

The Gardner equation [26] is developed to illustrate the description of solitary inner waves in shallow water and combines the KdV and modified KdV equations. The Gardner equation is frequently used in various branches of physics, such as plasma theories, quantum area theories, fluid mechanics, and physics [27].





Numerous wave phenomena in the plasma and solid phases are also covered [28]. We recognize the conformable fractional-order nonlinear Gardner (FG) equation in the following form:

$$\partial_t^\alpha w(x, t) + 6(w - \lambda^2 w^2) \frac{\partial w}{\partial x} - \frac{\partial^3 w}{\partial x^3} = 0, \quad (1)$$

with an initial condition

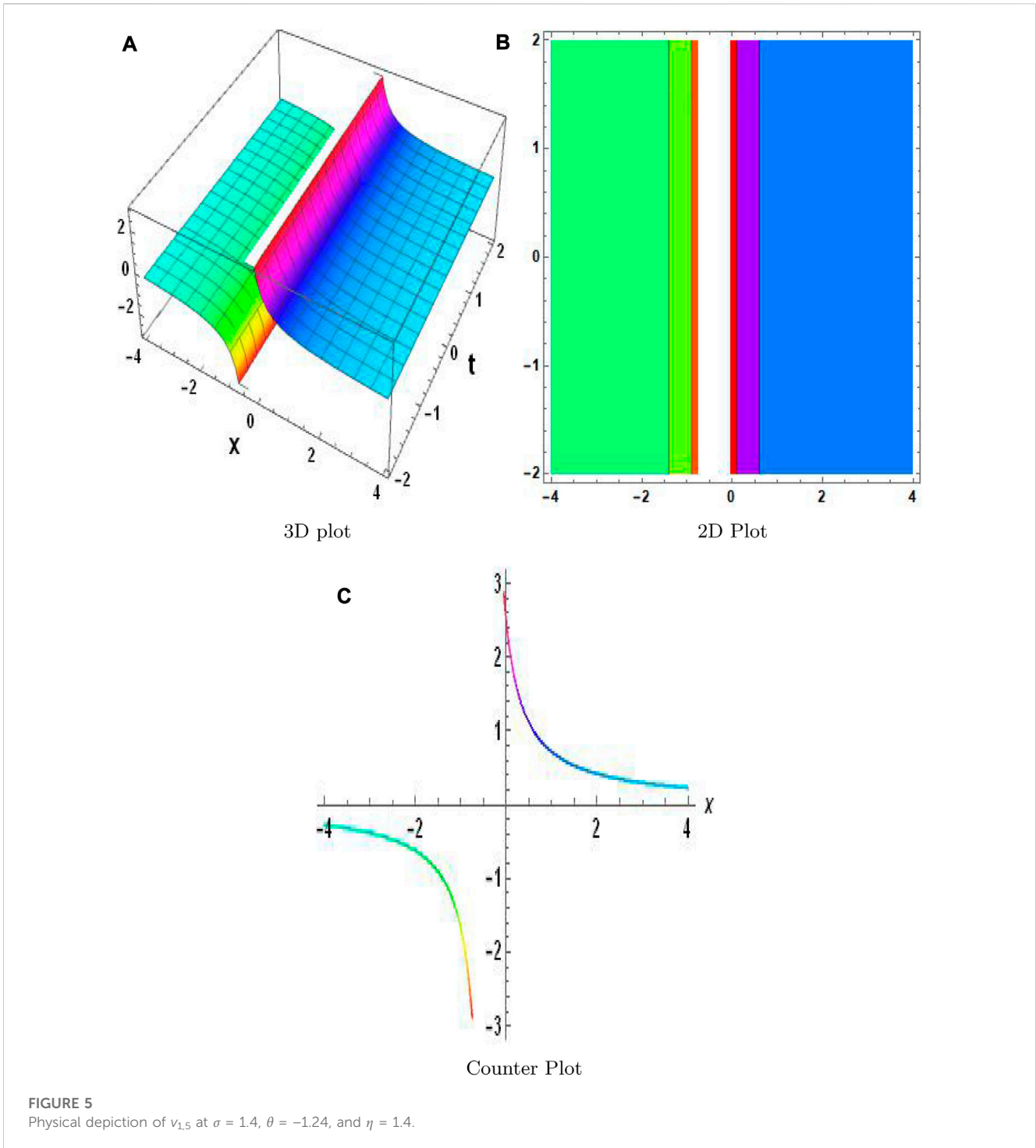
$$w(x, 0) = \frac{1}{2} + \frac{1}{2} \tanh\left(\frac{x}{2}\right),$$

and boundary condition

$$w(0, t) = \frac{1}{2} + \frac{1}{2} \tanh\left(\frac{-t}{2}\right),$$

$$w(1, t) = \frac{1}{2} + \frac{1}{2} \tanh\left(\frac{1-t}{2}\right).$$

A binary alloy's phase separation under a critical temperature is illustrated by the Cahn–Hilliard equation, which was first proposed by Cahn and Hilliard in 1958 [29]. The spinodal decomposition,



phase separation, and phase ordering dynamics are three fascinating physical phenomena that depend critically on this equation [30]. In this framework, the fractional Cahn–Hilliard (FCH) equation [31] is expressed as follows:

$$\partial_t^\alpha w(x, t) - \frac{\partial w}{\partial x} - 6w \left( \frac{\partial w}{\partial x} \right)^2 - (3w^2 - 1) \frac{\partial^2 w}{\partial x^2} + \frac{\partial^4 w}{\partial x^4} = 0, \quad (2)$$

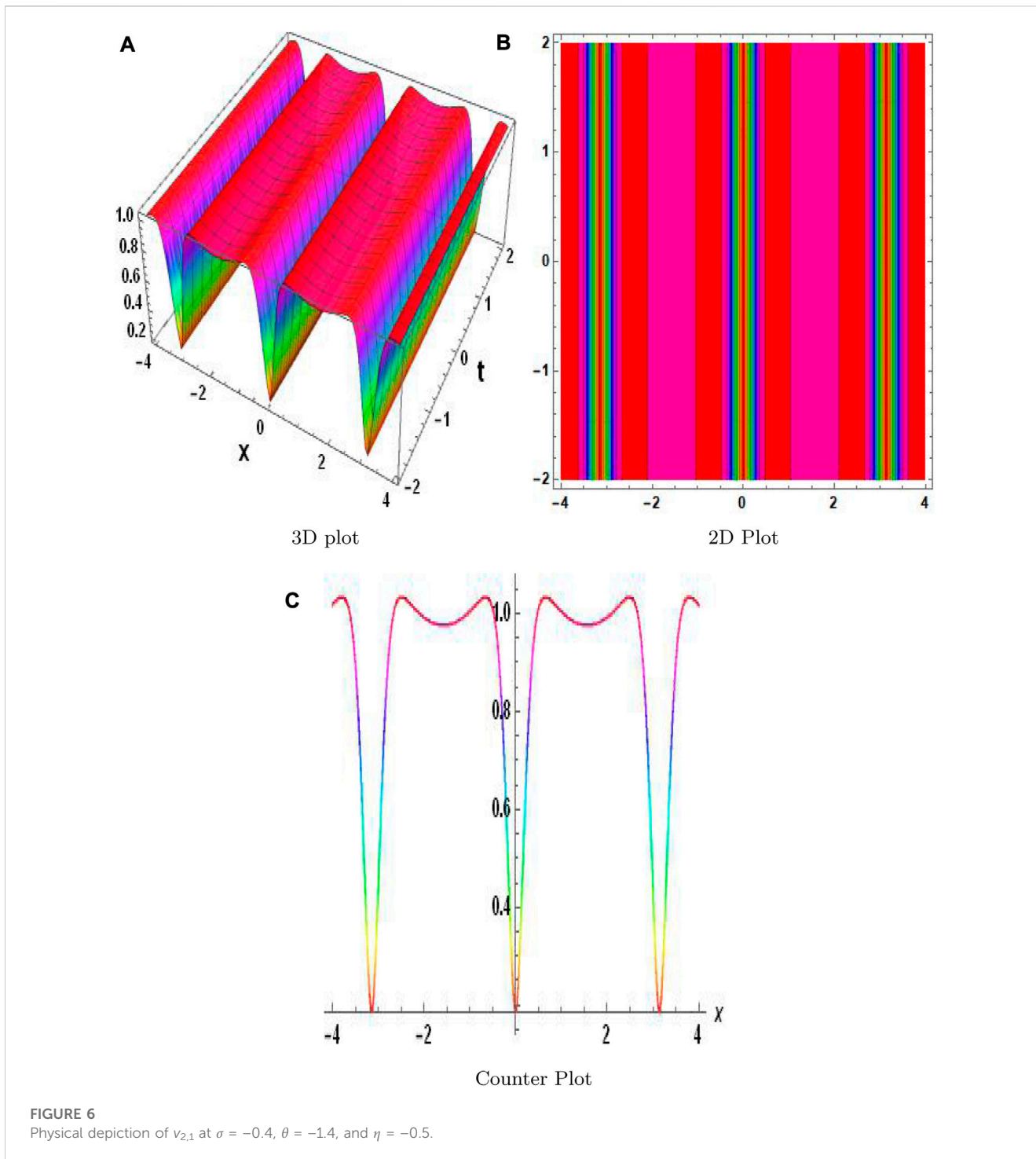
with an initial condition

$$w(x, 0) = \tanh\left(\frac{\sqrt{2}(x)}{2}\right),$$

and boundary condition

$$w(0, t) = \tanh\left(\frac{\sqrt{2}(t)}{2}\right),$$

$$w(1, t) = \tanh\left(\frac{\sqrt{2}(1+t)}{2}\right).$$



The methodology of this paper includes the following: [Section 2](#) discusses the modified auxiliary equation method (MAEM) and also solves the equations. [Section 3](#) discusses the semi-analytical fractional conformable residual power series algorithm and contains an explanation of the system to a solution. [Section 4](#) examines the stability property of the equations. [Section 5](#) contains the discussion and results of the system to illustrate the approximate delicacy. [Section 6](#) presents the conclusion.

**Preliminaries**

**Definition 1:** The  $\alpha$ -order fractional conformable derivative of a function  $w(x, t)$  of order  $\alpha \in (0, 1)$  is given as

$$\frac{\partial^\alpha w(t)}{\partial t} = \lim_{\epsilon \rightarrow 0} \frac{w(\epsilon t^{1-\alpha} + t) - w(t)}{\epsilon}, t > 0.$$

Moreover, if the previous limit exists at a point  $s$ ;  $s > 0$  in  $(0, s)$ , then  $w(t)$  is called  $\alpha$ -differentiable so that  $\frac{\partial^\alpha w(s)}{\partial t} = \lim_{t \rightarrow s^+} \frac{\partial^\alpha w(t)}{\partial t}$ .

**Definition 2:** The multiple time-fractional series (MTFS) expansion  $t_0 > 0$  is given as

$$\sum_{i=0}^{\infty} \zeta_i(x)(t - t_0)^{i\alpha} = \zeta_0(x) + \zeta_1(x)(t - t_0)^\alpha + \dots,$$



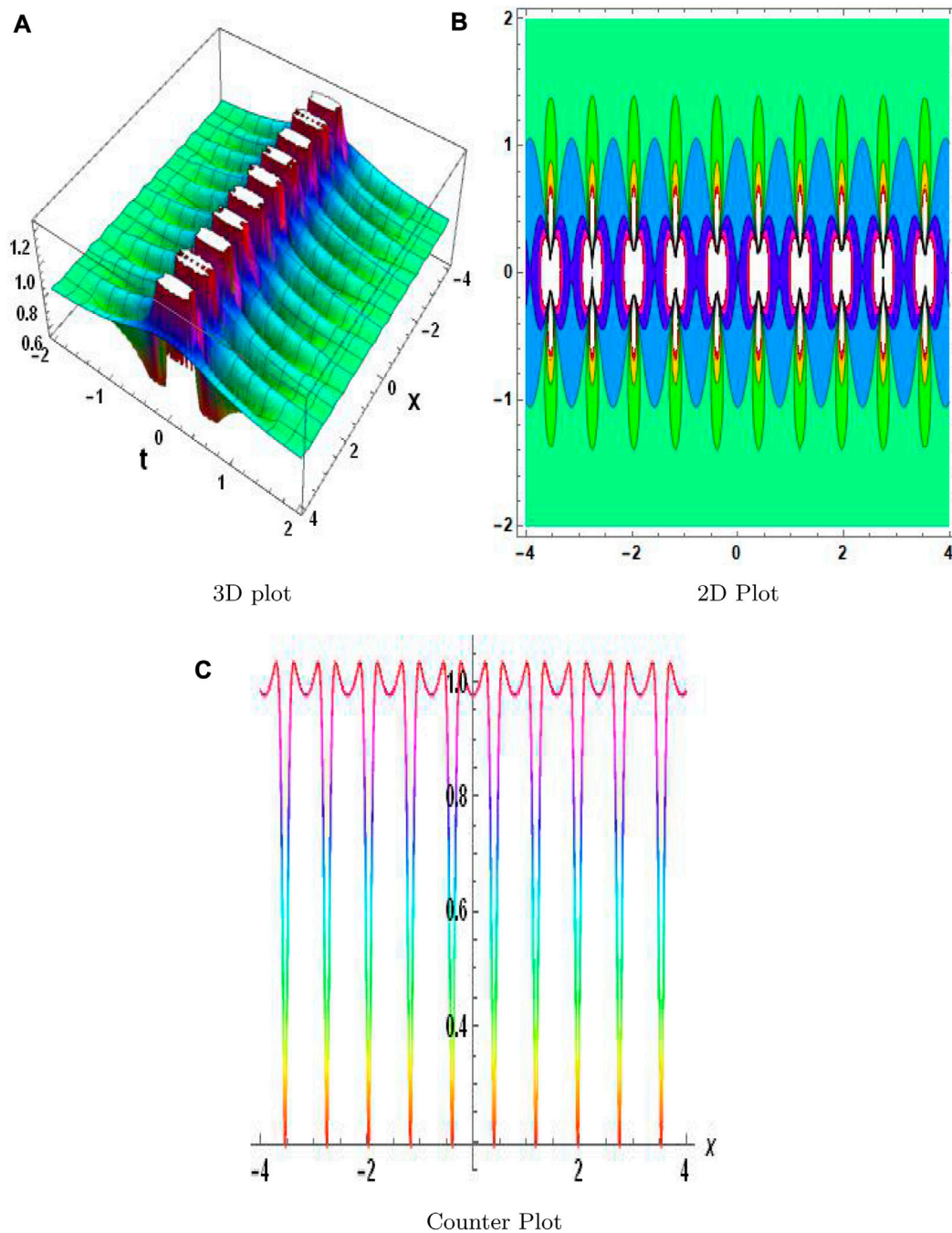


**FIGURE 7**  
Physical depiction of  $v_{2,2}$  at  $\sigma = 0.74$ ,  $\theta = -1.74$ , and  $\eta = 0.75$ .

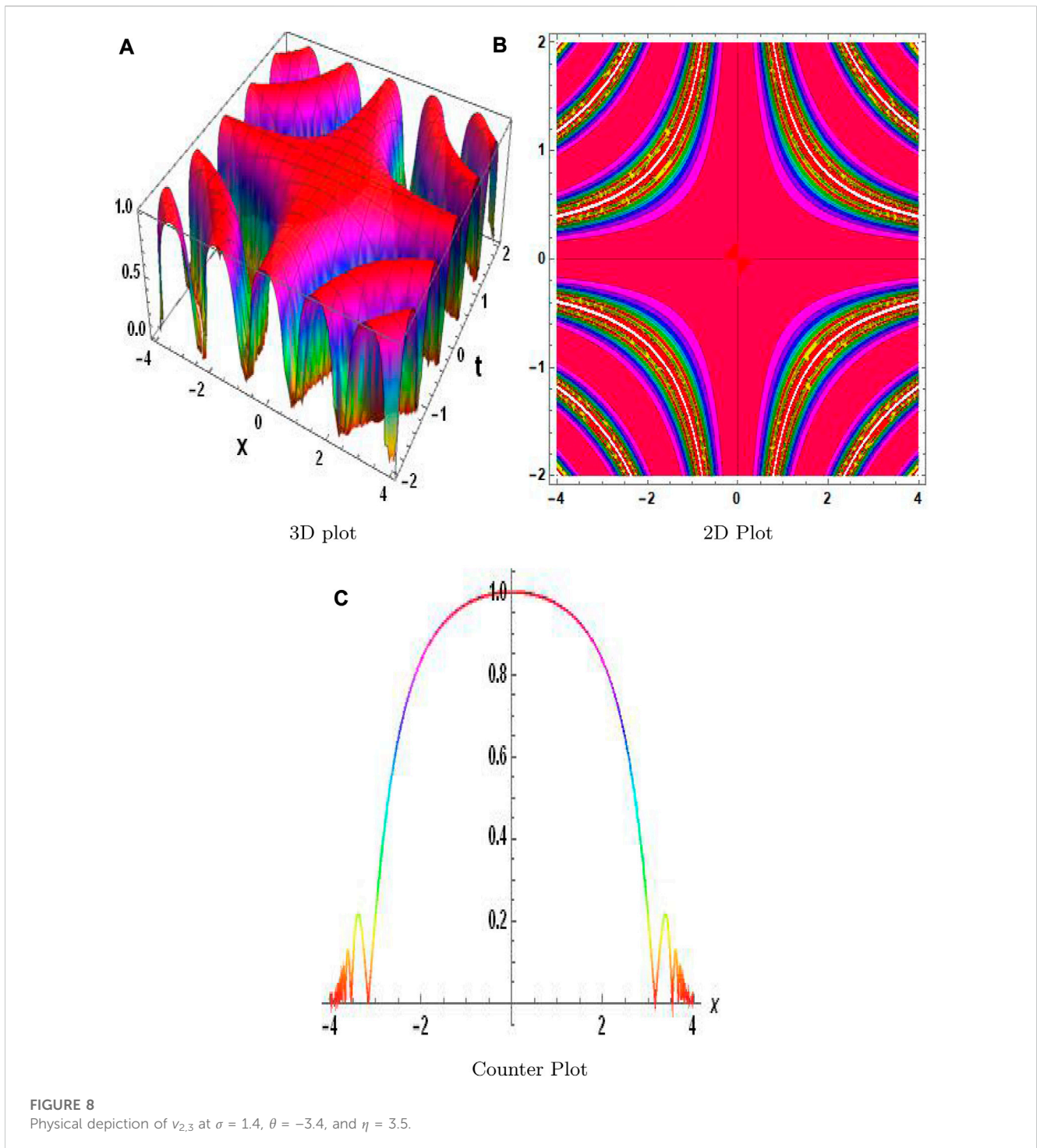
where  $\epsilon(n - 1, n)$ ,  $t \in (t_0, t_0 + r^{1/\alpha})$ ,  $r > 0$ ,  $r^{1/\alpha}$  is a radius of convergence and  $\zeta_i(x)$  indicates unknown coefficients of the expansion. When  $\alpha = 1$ , then the expansion in Definition 2 reduces to the usual series expansion at  $t_0 > 0$ , with a radius of convergence  $r$  that converges uniformly on  $|t - t_0| < r$ . Many other definitions are provided in [32].

## 2 Methodology

### 2.1 Modified auxiliary equation method

First, we introduce the MAEM [33]. Let us consider FNL PDEs.

$$F(v, v_t^\alpha, v_{xx}, v_{xt}, \dots) = 0, \tag{3}$$



where  $F$  is the function's polynomial. In Eq. 3,  $v$  is a function of the spatial variables  $x$  and  $t$  and represents the propagation of the wave profile. To modify the following, Eq. 3 is transformed into an ordinary differential equation as

$$v = V(\eta), \eta = x - \frac{vt^\alpha}{\alpha}, \tag{4}$$

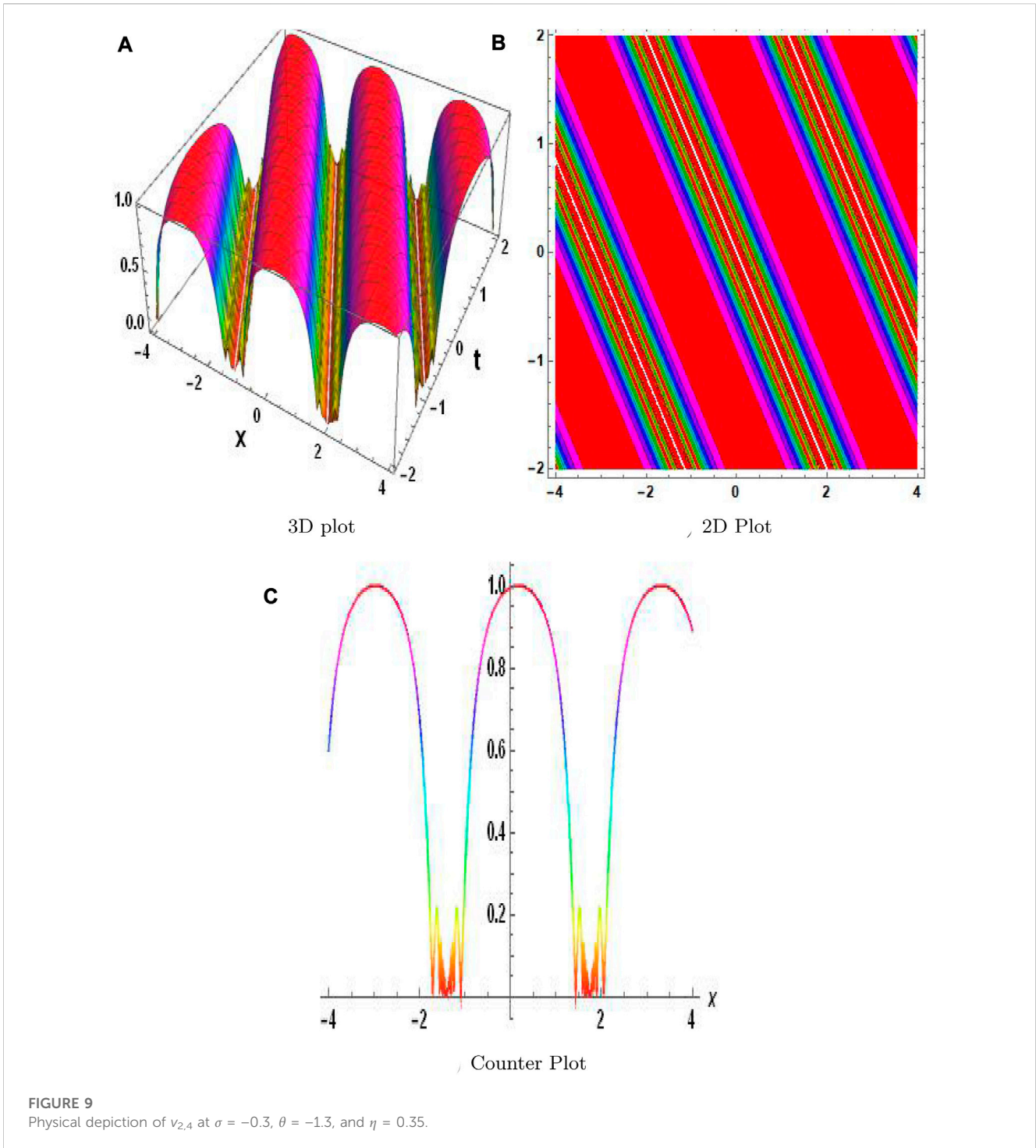
where  $\alpha$  represents arbitrary constants. Eq. 3 is converted into an ODE of the kind using transforms from Eq. 4.

$$M(V, V', V'', \dots) = 0, \tag{5}$$

where  $M$  stands for the polynomial involving the function  $V$  and its regular derivatives  $V' = dV/d\eta$ . The solution to Eq. 5 is

$$V(\eta) = a_0 + \sum_{i=1}^m (a_i L^{i\phi(\eta)} + a_{-i} (L)^{-i\phi(\eta)}), \tag{6}$$

where  $a_0$  and  $a_i$  are unknown constants. Function  $\phi'(\eta)$  is expressed as



$$\phi'(\eta) = \frac{\theta L^{\phi(\eta)} + \vartheta L^{-\phi(\eta)} + \sigma}{\ln(L)}, \quad (7)$$

where  $\sigma$ ,  $\theta$ , and  $\vartheta$  are arbitrary constants and  $L \neq 1, L > 0$ . On the basis of the (HBP), we may calculate  $N$ . The formal solution to Eq. 5 is obtained by replacing the  $N$  in Eq. 6. By substituting the ODE Eq. 7 formal solution into Eq. 5 and setting the coefficients of  $L^{i\phi(\eta)}$ ,  $i = 0, \pm 1, \pm 2 \dots$  to zero, the system of linear equations is produced. The unknown constants  $a_0$ ,  $a_p$  and  $a_{-i}$  can be found by solving this system of

equations. The following solutions for auxiliary Eq. 7 are taken into consideration as follows:

**Case I:** When  $\vartheta \neq 0, \sigma^2 - 4\theta\vartheta < 0$ ,

$$L^{\phi(\eta)} = \frac{-\sigma + \sqrt{-\sigma^2 + 4\theta\vartheta} \tan\left(\frac{1}{2} \sqrt{-\sigma^2 + 4\theta\vartheta} \eta\right)}{2\vartheta}, \quad (8)$$

or

$$L^{\phi(\eta)} = -\frac{\sigma + \sqrt{-\sigma^2 + 4\theta\vartheta} \cot\left(\frac{1}{2} \sqrt{-\sigma^2 + 4\theta\vartheta} \eta\right)}{2\vartheta}. \quad (9)$$

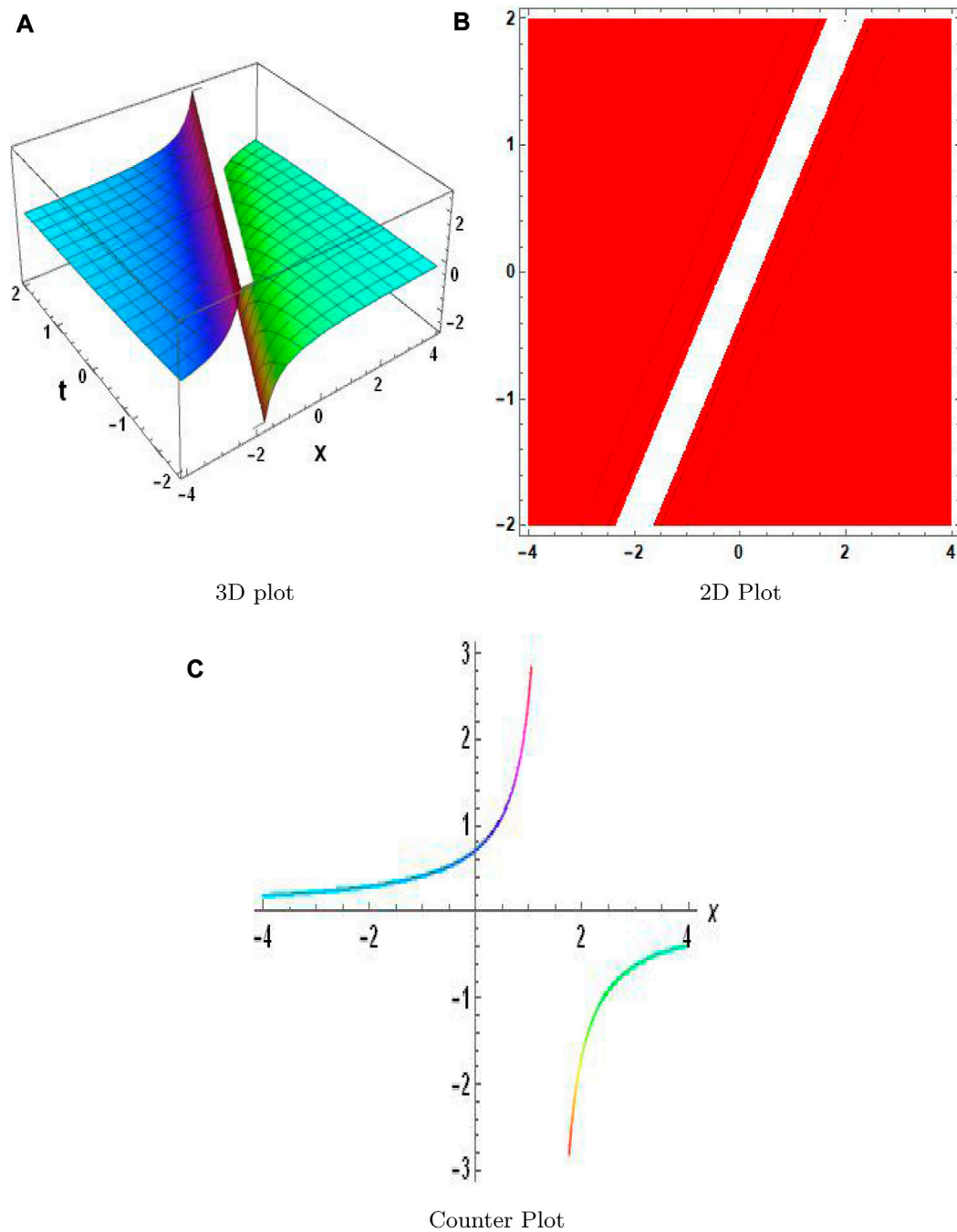


**FIGURE 10**  
Physical depiction of  $v_{2,5}$  at  $\sigma = 0.4$ ,  $\theta = -1.4$ , and  $\eta = 0.5$ . (A) is 3-D plot, (B) is 2-D plot, and (C) is contour plot.

**Case II:** When  $\vartheta \neq 0$ ,  $\sigma^2 - 4\theta\vartheta > 0$ ,

$$L^\phi(\eta) = -\frac{\sigma + \sqrt{-\sigma^2 + 4\theta\vartheta} \tanh\left(\frac{1}{2}\sqrt{-\sigma^2 + 4\theta\vartheta}\eta\right)}{2\vartheta}, \quad (10)$$

or

$$L^\phi(\eta) = -\frac{\sigma + \sqrt{-\sigma^2 + 4\theta\vartheta} \coth\left(\frac{1}{2}\sqrt{-\sigma^2 + 4\theta\vartheta}\eta\right)}{2\vartheta}. \quad (11)$$

**Case III:** When  $\vartheta \neq 0$ ,  $\sigma^2 - 4\theta\vartheta = 0$ ,

$$L^\phi(\eta) = -\frac{\sigma\eta + 2}{2\vartheta\eta}. \quad (12)$$

By substituting the unknown values for  $a_0$ ,  $a_i$ ,  $a_{.i}$  and the aforementioned cases into Eq. 6, using transformations from Eq. 4, it is possible to obtain the closed-form solutions to Eq. 1 and Eq. 2.



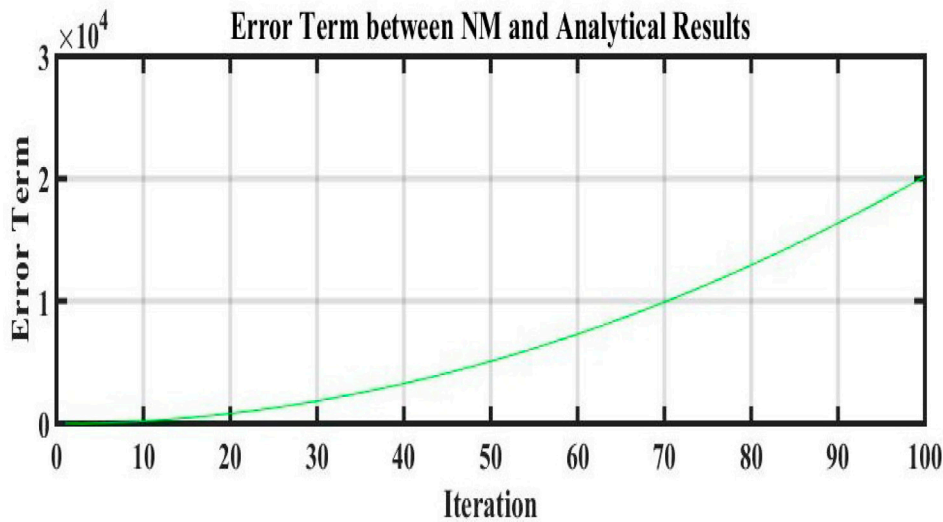


**FIGURE 11**  
Comparison of error terms between numerical and analytical results by using values of Table 1.

### 2.1.1 Application to the fractional-order nonlinear Gardner equation

The governing Eq. 1 transforms into the following ODE using the following conformable derivative transformation from Eq. 4:

$$\begin{aligned} -\nu V' + V^{(3)} + 6(V - \lambda^2 V^2)V' &= 0, \\ -\nu V + V'' - 2\lambda^2 V^3 + 3V^2 &= 0. \end{aligned} \tag{13}$$

By changing the degree of the highest-order derivative term and nonlinear with HBP,  $N = 1$  is calculated. According to the formal solution in Eq. 13 derived from Eq. 6, we obtain

$$V(\eta) = a_0 + a_1 L^\phi(\eta) + \frac{a_{-1}}{L^\phi(\eta)}. \tag{14}$$

When Eq. 14 is substituted with Eq. 7 in Eq. 13, the coefficients of powers of  $L^{i\phi(\eta)}$ ,  $i = 0, \pm 1, \pm 2 \dots$  are set to zero, resulting in a linear equation system. The following sets of solutions are found by using Mathematica software.

**Set 1:**

$$a_1 = 0, a_{-1} = \frac{\vartheta}{\lambda}, a_0 = 0, \nu = \frac{1}{\lambda^2}, \theta = 0, \sigma = -\frac{1}{\lambda}. \tag{15}$$

**Set 2:**

$$a_1 = -\frac{1}{16\lambda^3\vartheta}, a_{-1} = -\frac{\vartheta}{\lambda}, a_0 = \frac{1}{2\lambda^2}, \nu = \frac{1}{\lambda^2}, \theta = -\frac{1}{16\lambda^2\vartheta}, \sigma = 0. \tag{16}$$

**Set 3:**

$$a_1 = \frac{1}{16\lambda^3\vartheta}, a_{-1} = \frac{\vartheta}{\lambda}, a_0 = \frac{1}{2\lambda^2}, \nu = \frac{1}{\lambda^2}, \theta = -\frac{1}{16\lambda^2\vartheta}, \sigma = 0. \tag{17}$$

**Set 4:**

$$a_1 = 0, a_{-1} = -\frac{\vartheta}{\lambda}, a_0 = \frac{1}{\lambda^2}, \nu = \frac{1}{\lambda^2}, \theta = 0, \sigma = -\frac{1}{\lambda}. \tag{18}$$

**Set 5:**

$$a_1 = 0, a_{-1} = \frac{\vartheta}{\lambda}, a_0 = \frac{1}{\lambda^2}, \nu = \frac{1}{\lambda^2}, \theta = 0, \sigma = \frac{1}{\lambda}. \tag{19}$$

**Family 1.** Solutions to Eq. 1 are derived by substituting the values from Set 1 into Eq. 15.

**Case I:** When  $\vartheta \neq 0, \sigma^2 - 4\theta\vartheta < 0$ ,

$$v_{1,1} = \frac{2\vartheta^2}{\lambda \left( \sqrt{4\theta\vartheta - \sigma^2} \tan\left(\frac{1}{2}\eta\sqrt{4\theta\vartheta - \sigma^2}\right) - \sigma \right)}, \tag{20}$$

or

$$v_{1,2} = -\frac{2\vartheta^2}{\lambda \left( \sqrt{4\theta\vartheta - \sigma^2} \cot\left(\frac{1}{2}\eta\sqrt{4\theta\vartheta - \sigma^2}\right) + \sigma \right)}. \tag{21}$$

**Case II:** When  $\vartheta \neq 0, \sigma^2 - 4\theta\vartheta > 0$ ,

$$v_{1,3} = -\frac{2\vartheta^2}{\lambda \left( \sqrt{4\theta\vartheta - \sigma^2} \tanh\left(\frac{1}{2}\eta\sqrt{4\theta\vartheta - \sigma^2}\right) + \sigma \right)}, \tag{22}$$

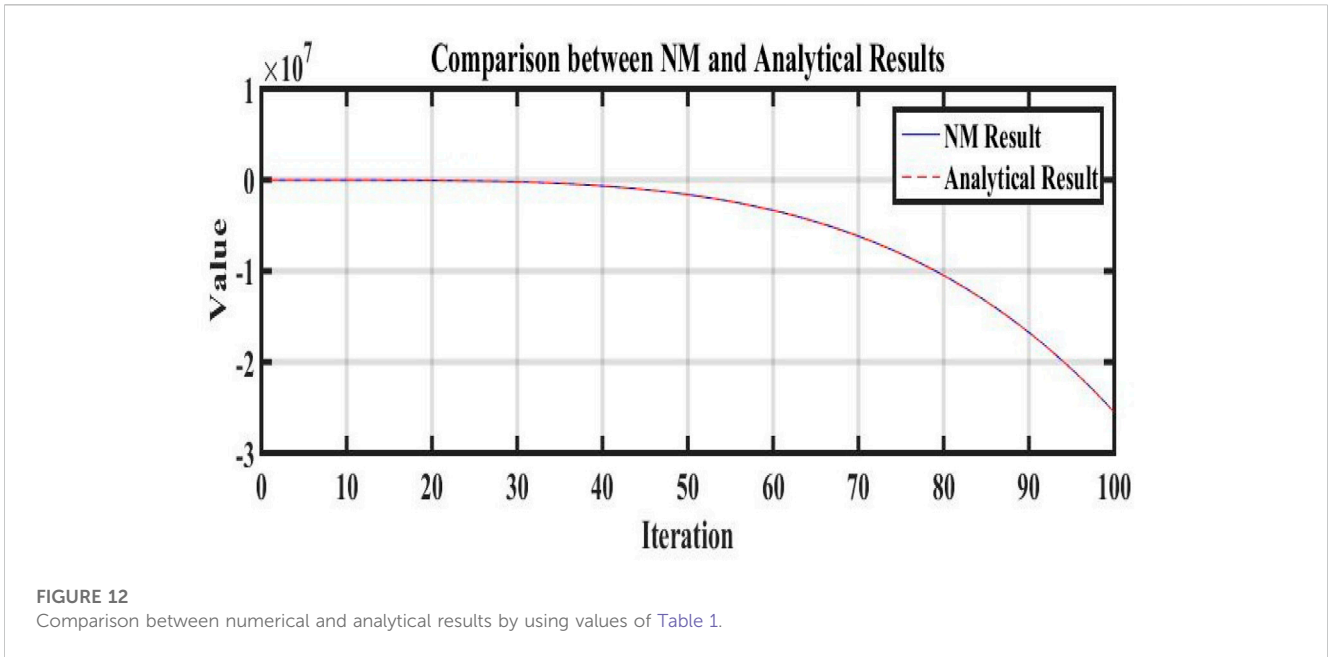
or

$$v_{1,4} = -\frac{2\vartheta^2}{\lambda \left( \sqrt{4\theta\vartheta - \sigma^2} \coth\left(\frac{1}{2}\eta\sqrt{4\theta\vartheta - \sigma^2}\right) + \sigma \right)}. \tag{23}$$

**Case III:** When  $\vartheta \neq 0, \sigma^2 - 4\theta\vartheta = 0$ ,

$$v_{1,5} = -\frac{2\vartheta^2 \left( x - \frac{t^\alpha}{\alpha\lambda^2} \right)}{\lambda \left( 2 - \frac{x - \frac{t^\alpha}{\alpha\lambda^2}}{\lambda} \right)}. \tag{24}$$





**Family 2.** Solutions to Eq. 1 are derived by substituting the values from Set 2 into Eq. 16.

**Case I:** When  $\vartheta \neq 0, \sigma^2 - 4\theta\vartheta < 0,$

$$v_{1,6} = \frac{1}{2\lambda^2} - \frac{\sqrt{4\theta\vartheta - \sigma^2} \tan\left(\frac{1}{2}\eta\sqrt{4\theta\vartheta - \sigma^2}\right) - \sigma}{32\lambda^3\vartheta^2} - \frac{\lambda\left(\sqrt{4\theta\vartheta - \sigma^2} \tan\left(\frac{1}{2}\eta\sqrt{4\theta\vartheta - \sigma^2}\right) - \sigma\right)}{2\vartheta^2} \tag{25}$$

or

$$v_{1,7} = \frac{1}{2\lambda^2} + \frac{\sqrt{4\theta\vartheta - \sigma^2} \cot\left(\frac{1}{2}\eta\sqrt{4\theta\vartheta - \sigma^2}\right) + \sigma}{32\lambda^3\vartheta^2} + \frac{\lambda\left(\sqrt{4\theta\vartheta - \sigma^2} \cot\left(\frac{1}{2}\eta\sqrt{4\theta\vartheta - \sigma^2}\right) + \sigma\right)}{2\vartheta^2}$$

**Case II:** When  $\vartheta \neq 0, \sigma^2 - 4\theta\vartheta > 0,$

$$v_{1,8} = \frac{1}{2\lambda^2} + \frac{\sqrt{4\theta\vartheta - \sigma^2} \tanh\left(\frac{1}{2}\eta\sqrt{4\theta\vartheta - \sigma^2}\right) + \sigma}{32\lambda^3\vartheta^2} + \frac{\lambda\left(\sqrt{4\theta\vartheta - \sigma^2} \tanh\left(\frac{1}{2}\eta\sqrt{4\theta\vartheta - \sigma^2}\right) + \sigma\right)}{2\vartheta^2} \tag{27}$$

or

$$v_{1,9} = \frac{1}{2\lambda^2} + \frac{\sqrt{4\theta\vartheta - \sigma^2} \coth\left(\frac{1}{2}\eta\sqrt{4\theta\vartheta - \sigma^2}\right) + \sigma}{32\lambda^3\vartheta^2} + \frac{\lambda\left(\sqrt{4\theta\vartheta - \sigma^2} \coth\left(\frac{1}{2}\eta\sqrt{4\theta\vartheta - \sigma^2}\right) + \sigma\right)}{2\vartheta^2} \tag{28}$$

**Case III:** When  $\vartheta \neq 0, \sigma^2 - 4\theta\vartheta = 0,$

$$v_{1,10} = \frac{1}{2\lambda^2} + \frac{2\vartheta^2\left(x - \frac{t^\alpha}{\alpha\lambda^2}\right)}{\lambda\left(\sigma\left(x - \frac{t^\alpha}{\alpha\lambda^2}\right) + 2\right)} + \frac{\sigma\left(x - \frac{t^\alpha}{\alpha\lambda^2}\right) + 2}{32\lambda^3\vartheta^2\left(x - \frac{t^\alpha}{\alpha\lambda^2}\right)} \tag{29}$$

### 2.1.2 Application to the fractional-order nonlinear Cahn–Hilliard equation

The governing Eq. 2 transforms into the following ODE using the traveling wave transformations from Eq. 4:

$$-vV' + V^{(4)} - (3V^2 - 1)V'' - 6VV'^2 - V' = 0.$$

Then, integrating the aforementioned equation, we obtain

$$(-v - 1)V + V^{(3)} + (1 - 3V^2)V' = 0. \tag{30}$$

By adjusting the highest-order derivative term's degree and nonlinear using homogeneous balance principal,  $N = 1$  is calculated. According to the formal solution of Eq. 30 derived from Eq. 6, we obtain

$$V(\eta) = a_0 + a_1L^\phi(\eta) + \frac{a_{-1}}{L^\phi(\eta)}. \tag{31}$$

When Eq. 31 is substituted with Eq. 7 into Eq. 30, the coefficients of powers of  $L^{i\phi(\eta)}, i = 0, \pm 1, \pm 2 \dots$  are set to zero, resulting in a linear equation system. The following sets of solutions are found using Mathematica software.

**Set 1:**

$$a_1 = -\frac{5\sqrt{3}}{32\vartheta}, a_{-1} = -\frac{2\vartheta}{\sqrt{3}}, a_0 = \frac{1}{4\sqrt{3}}, v = -1, \sigma = 0, \theta = -\frac{15}{64\vartheta} \tag{32}$$

**Set 2:**

$$a_1 = 0, a_{-1} = \frac{2\vartheta}{\sqrt{3}}, a_0 = \frac{1}{27}(4\sqrt{3} - 5\sqrt{30}), v = -1, \sigma = \frac{1}{9}(5 - 4\sqrt{10}), \theta = 0. \tag{33}$$

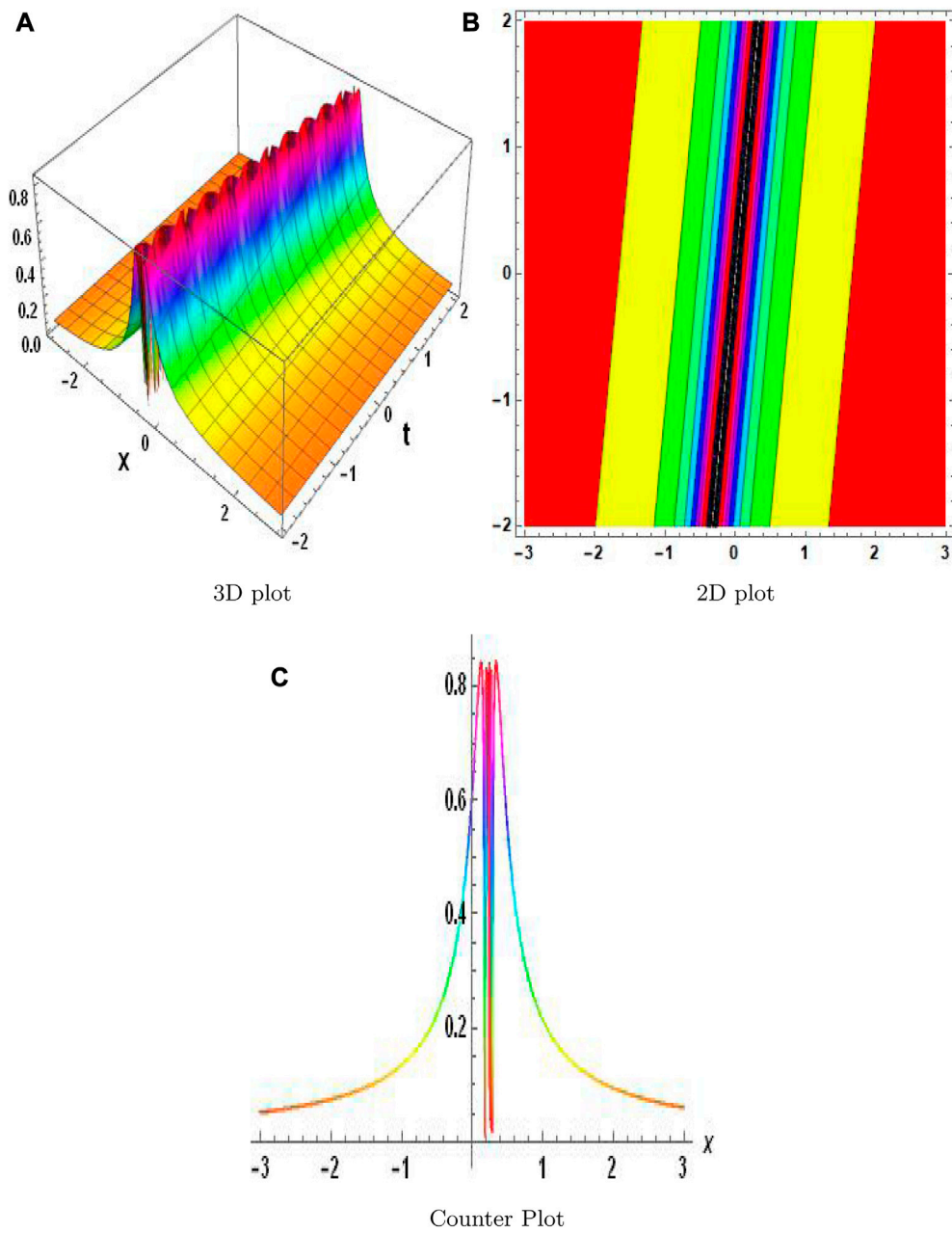


**FIGURE 13**  
Physical depiction of  $H$  in Eq. 92 under  $\sigma = 0.5$ ,  $\nu = 2.4$ ,  $\lambda = 1.4$ , and  $\vartheta = 0.4$ .

**Set 3:**

$$a_1 = \frac{5\sqrt{3}}{32\vartheta}, a_{-1} = \frac{2\vartheta}{\sqrt{3}}, a_0 = -\frac{1}{4\sqrt{3}}, \nu = -1, \sigma = 0, \theta = -\frac{15}{64\vartheta^2}$$

**Set 4:**

$$a_1 = 0, a_{-1} = \frac{2\vartheta}{\sqrt{3}}, a_0 = \frac{1}{27}(4\sqrt{3} + 5\sqrt{30}), \nu = -1, \sigma = \frac{1}{9}(4\sqrt{10} + 5), \theta = 0.$$

**Set 5:**

$$a_1 = 0, a_{-1} = -\frac{2\vartheta}{\sqrt{3}}, a_0 = \frac{1}{27}(5\sqrt{30} - 4\sqrt{3}), \nu = -1, \sigma = \frac{1}{9}(5 - 4\sqrt{10}), \theta = 0.$$

**Family 1.** Solutions to Eq. 2 are derived by substituting the values from Set 1 into Eq. 32.

**Case I:** When  $\vartheta \neq 0$ ,  $\sigma^2 - 4\theta\vartheta < 0$ ,

$$v_{2,1} = \frac{1}{4\sqrt{3}} - \frac{4\vartheta^2}{\sqrt{3}\left(\sqrt{4\theta\vartheta - \sigma^2} \tan\left(\frac{1}{2}\eta\sqrt{4\theta\vartheta - \sigma^2}\right) - \sigma\right)} - \frac{5\sqrt{3}\left(\sqrt{4\theta\vartheta - \sigma^2} \tan\left(\frac{1}{2}\eta\sqrt{4\theta\vartheta - \sigma^2}\right) - \sigma\right)}{64\vartheta^2}, \tag{34}$$

or

$$v_{2,2} = \frac{1}{4\sqrt{3}} + \frac{4\vartheta^2}{\sqrt{3}\left(\sqrt{4\theta\vartheta - \sigma^2} \cot\left(\frac{1}{2}\eta\sqrt{4\theta\vartheta - \sigma^2}\right) + \sigma\right)} + \frac{5\sqrt{3}\left(\sqrt{4\theta\vartheta - \sigma^2} \cot\left(\frac{1}{2}\eta\sqrt{4\theta\vartheta - \sigma^2}\right) + \sigma\right)}{64\vartheta^2}. \tag{35}$$

Case II: When  $\vartheta \neq 0, \sigma^2 - 4\theta\vartheta > 0,$

$$v_{2,3} = \frac{1}{4\sqrt{3}} + \frac{4\vartheta^2}{\sqrt{3}\left(\sqrt{4\theta\vartheta - \sigma^2} \tanh\left(\frac{1}{2}\eta\sqrt{4\theta\vartheta - \sigma^2}\right) + \sigma\right)} + \frac{5\sqrt{3}\left(\sqrt{4\theta\vartheta - \sigma^2} \tanh\left(\frac{1}{2}\eta\sqrt{4\theta\vartheta - \sigma^2}\right) + \sigma\right)}{64\vartheta^2}, \tag{36}$$

or

$$v_{2,4} = \frac{1}{4\sqrt{3}} + \frac{4\vartheta^2}{\sqrt{3}\left(\sqrt{4\theta\vartheta - \sigma^2} \coth\left(\frac{1}{2}\eta\sqrt{4\theta\vartheta - \sigma^2}\right) + \sigma\right)} + \frac{5\sqrt{3}\left(\sqrt{4\theta\vartheta - \sigma^2} \coth\left(\frac{1}{2}\eta\sqrt{4\theta\vartheta - \sigma^2}\right) + \sigma\right)}{64\vartheta^2}. \tag{37}$$

Case III: When  $\vartheta \neq 0, \sigma^2 - 4\theta\vartheta = 0,$

$$v_{2,5} = \frac{1}{4\sqrt{3}} + \frac{4\eta\vartheta^2}{\sqrt{3}(\eta\sigma + 2)} + \frac{5\sqrt{3}(\eta\sigma + 2)}{64\eta\vartheta^2}. \tag{38}$$

### 3 Numerical investigation using the fractional conformable residual power series algorithm

In this section, a newly developed approach is utilized to produce accurate approximations of the time-fractional equations supplied with a given initial condition inside a finite spatiotemporal domain [34]. This approach uses a newly designed algorithm. Let us consider the following nonlinear time-fractional equations to achieve our goal:

$$\partial_t^\alpha w(x, t) + N(w, w^2, w_x, w_{xx}) + \dots = 0, \tag{39}$$

with an initial condition

$$w(x, 0) = w_0(x). \tag{40}$$

The numerical simulation that is being provided assumes that the solution to Eqs 39, 40 has a multiple time-fractional series (MTFS) expansion of approximately  $t_0 = 0$  of the following form:

$$w(x, t) = \sum_{i=1}^m \frac{t^{i\alpha} \zeta_i(x)}{i! \alpha^i}. \tag{41}$$

The  $m$ th truncated solution of  $w(x, t)$  of Eq. 40 is defined as

$$w_m = \zeta_0(x) + \sum_{i=1}^m \frac{t^{i\alpha} \zeta_i(x)}{i! \alpha^i}. \tag{42}$$

Initially, the residual error  $R_s(x, t)$  of Eqs 39, 40 is given as

$$\mathcal{R}_s(x, t) = \partial_t^\alpha w(x, t) + N(w, w^2, w_x, w_{xx}) + \dots \tag{43}$$

The  $R_s(x, t)$   $m$ th residual error should be truncated so that

$$\mathcal{R}_s^m(x, t) = \partial_t^\alpha w_m(x, t) + N(w_m, w_m^2, w_{x,m}, w_{xx,m}) + \dots \tag{44}$$

By replacing the  $m$ th truncated residual error in Eq. 44 with the truncated MTFS solution in Eq. 42, we obtain

$$\begin{aligned} \partial_t^{\alpha(m-1)} \mathcal{R}_s^2(x, t) &= \partial_t^{m\alpha} \left( \zeta_0(x) + \sum_{i=1}^m \frac{t^{i\alpha} \zeta_i(x)}{i! \alpha^i} \right) \\ &+ N \left( \left( \sum_{i=1}^m \frac{t^{i\alpha} \zeta_i(x)}{i! \alpha^i} + \zeta_0(x) \right) \right), \\ &N \left( \left( \sum_{i=1}^m \frac{t^{i\alpha} \zeta_i(x)}{i! \alpha^i} + \zeta_0(x) \right)^2, \right. \\ &\left. \left( \sum_{i=1}^m \frac{t^{i\alpha} \zeta_i(x)}{i! \alpha^i} + \zeta_0(x) \right)_x, \right. \\ &\left. \left( \sum_{i=1}^m \frac{t^{i\alpha} \zeta_i(x)}{i! \alpha^i} + \zeta_0(x) \right)_{xx} \right) + \dots \end{aligned} \tag{45}$$

To make the major steps of the provided FCRPSA in determining the  $m$ -term truncated solution's unknown coefficients  $\zeta_i(x)$  more clear (Eq. 42), set  $m = 1$  and equate  $R_s^1(x, t)$  to zero at  $t = 0$ . Therefore,  $\zeta_1(x)$  is obtained. Thereafter, set  $m = 2$ , apply operator  $\partial_t^\alpha$  on both sides of the resulting relevant equation, and solve  $\partial_t^\alpha \mathcal{R}_s^2(x, 0)$ . Then,  $\zeta_2(x)$  is also obtained. The unknown coefficient  $\zeta_i(x)$  of the MTFS expansion would be discovered if we continue solving in this manner (Eq. 42).

### 3.1 Numerical simulation of the fractional-order nonlinear Gardner equation

Let us consider the equation

$$D_t^\alpha w(x, t) + 6(w - \lambda^2 w^2) \frac{\partial w}{\partial x} - \frac{\partial^3 w}{\partial x^3} = 0, \tag{46}$$

with an initial condition

$$w(0, t) = \frac{1}{2} \tanh\left(\frac{x}{2}\right) + \frac{1}{2}. \tag{47}$$

We use the fractional conformable residual power series algorithm to solve this equation. For this, the  $m$ -truncated term is taken as

$$w_m = \zeta_0(x) + \sum_{i=1}^m \frac{t^{i\alpha} \zeta_i(x)}{i! \alpha^i}, \tag{48}$$

and the residual error function is

$$\mathcal{R}_s^m(x, t) = \frac{\partial^\alpha w_m}{\partial t} + 6w_m - \lambda^2 w_m^2 \frac{\partial w_m}{\partial x} + \frac{\partial^3 w_m}{\partial x^3}. \tag{49}$$

For  $m = 0,$

$$w_0(x, t) = \frac{1}{2} \tanh\left(\frac{x}{2}\right) + \frac{1}{2}.$$

For  $m = 1$ , the truncated term is

$$w_1(x, t) = \zeta_0(x) + \frac{\zeta_1(x)t^\alpha}{\alpha}, \tag{50}$$

$$\zeta_0(x) = w_0(x, t) = \frac{1}{2} \tanh\left(\frac{x}{2}\right) + \frac{1}{2}, \tag{51}$$

$$w_1(x, t) = \frac{1}{2} \tanh\left(\frac{x}{2}\right) + \frac{1}{2} + \frac{\zeta_1(x)t^\alpha}{\alpha}. \tag{52}$$

Therefore, the first residual error function is

$$\mathcal{R}_s^1(x, t) = \frac{\partial^\alpha w_1}{\partial t} + 6w_1 - \lambda^2 w_1^2 \frac{\partial w_1}{\partial x} + \frac{\partial^3 w_1}{\partial x^3}. \tag{53}$$

Substituting Eq. 50 into Eq. 53, we obtain

$$\begin{aligned} \mathcal{R}_s^1(x, t) = & 6\left(\left(\frac{t^\alpha \zeta_1(x)}{\alpha} + \zeta_0(x)\right) - \lambda^2 \left(\frac{t^\alpha \zeta_1(x)}{\alpha} + \zeta_0(x)\right)^2\right) \\ & \left(\frac{t^\alpha \zeta_1'(x)}{\alpha} + \zeta_0'(x)\right) + \left(\frac{t^\alpha \zeta_1^3(x)}{\alpha} + \zeta_0^3(x)\right) + \zeta_1(x). \end{aligned} \tag{54}$$

Thus,  $\mathcal{R}_s^1(x, t)$  at  $t = 0$  results in

$$6(\zeta_0(x) - \lambda^2 \zeta_0(x)^2) \zeta_0'(x) + \zeta_0^3(x) + \zeta_1(x) = 0, \tag{55}$$

$$\zeta_1(x) = \frac{1}{8} \operatorname{sech}^4\left(\frac{x}{2}\right) (3(\lambda^2 - 1) \sinh(x) + (3\lambda^2 - 4) \cosh(x) - 1). \tag{56}$$

So, the first series solution  $w_1(x, t)$  is provided by

$$w_1(x, t) = \frac{1}{2} + \frac{1}{2} \tanh\left(\frac{x}{2}\right) + \frac{1}{8} \operatorname{sech}^4\left(\frac{x}{2}\right) \times (3(\lambda^2 - 1) \sinh(x) + (3\lambda^2 - 4) \cosh(x) - 1) \frac{t^\alpha}{\alpha}. \tag{57}$$

For  $m = 2$ , the truncated term is

$$w_2(x, t) = \frac{\zeta_2(x)t^{2\alpha}}{2\alpha^2} + \frac{\zeta_1(x)t^\alpha}{\alpha} + \zeta_0(x), \tag{58}$$

$$\begin{aligned} w_2(x, t) = & \frac{1}{2} + \frac{1}{2} \tanh\left(\frac{x}{2}\right) + \frac{1}{8} \operatorname{sech}^4\left(\frac{x}{2}\right) \\ & \times (3(\lambda^2 - 1) \sinh(x) + (3\lambda^2 - 4) \cosh(x) - 1) \frac{t^\alpha}{\alpha} \\ & + \frac{\zeta_2(x)t^{2\alpha}}{2\alpha^2}, \end{aligned} \tag{59}$$

and the second residual error function is obtained by substituting Eq. 58 into Eq. 59

$$\begin{aligned} \mathcal{R}_s^2(x, t) = & \frac{\partial^\alpha}{\partial t} \left( \frac{t^{2\alpha} \zeta_2(x)}{2\alpha^2} + \frac{t^\alpha \zeta_1(x)}{\alpha} + \zeta_0(x) \right) \\ & + 6 \left( \left( \frac{t^{2\alpha} \zeta_2(x)}{2\alpha^2} + \frac{t^\alpha \zeta_1(x)}{\alpha} + \zeta_0(x) \right) \right. \\ & \left. - \lambda^2 \left( \frac{t^{2\alpha} \zeta_2(x)}{2\alpha^2} + \frac{t^\alpha \zeta_1(x)}{\alpha} + \zeta_0(x) \right)^2 \right) \\ & \frac{\partial^2}{\partial x^2} \left( \frac{t^{2\alpha} \zeta_2(x)}{2\alpha^2} + \frac{t^\alpha \zeta_1(x)}{\alpha} + \zeta_0(x) \right) \\ & + \frac{\partial^3}{\partial x^3} \left( \frac{t^{2\alpha} \zeta_2(x)}{2\alpha^2} + \frac{t^\alpha \zeta_1(x)}{\alpha} + \zeta_0(x) \right), \end{aligned} \tag{60}$$

$$\begin{aligned} \mathcal{R}_s^2(x, t) = & \left( \frac{t^\alpha \zeta_2(x)}{\alpha} + \zeta_1(x) \right) \\ & + 6 \left( \left( \frac{t^{2\alpha} \zeta_2(x)}{2\alpha^2} + \frac{t^\alpha \zeta_1(x)}{\alpha} + \zeta_0(x) \right) \right. \\ & \left. - 6\lambda^2 \left( \frac{t^{2\alpha} \zeta_2(x)}{2\alpha^2} + \frac{t^\alpha \zeta_1(x)}{\alpha} + \zeta_0(x) \right)^2 \right) \\ & \left( \frac{t^{2\alpha} \zeta_2'(x)}{2\alpha^2} + \frac{t^\alpha \zeta_1'(x)}{\alpha} + \zeta_0'(x) \right) \\ & + \left( \frac{t^{2\alpha} \zeta_2^3(x)}{2\alpha^2} + \frac{t^\alpha \zeta_1^3(x)}{\alpha} + \zeta_0^3(x) \right). \end{aligned} \tag{61}$$

Then,  $d^\alpha/dt$  is applied on both sides of Eq. 61 and thus at  $t = 0$ , we obtain

$$(-\zeta_1^3(x)) (\zeta_2(x) = 12\lambda^2 \zeta_0(x) \zeta_1(x) \zeta_0'(x) + 6\lambda^2 \zeta_0(x)^2 \zeta_1'(x) - 6\zeta_1(x) \zeta_0'(x) - 6\zeta_0(x) \zeta_1'(x)), \tag{62}$$

$$\begin{aligned} \zeta_2(x) = & -\frac{1}{64} \operatorname{sech}^7\left(\frac{x}{2}\right) \left( 18\lambda^4 \cosh\left(\frac{5x}{2}\right) - 42\lambda^2 \cosh\left(\frac{5x}{2}\right) \right. \\ & \left. - 24(\lambda^2 - 1) \cosh\left(\frac{x}{2}\right) \right) - \frac{1}{64} \operatorname{sech}^7\left(\frac{x}{2}\right) \\ & \left( -6(15\lambda^4 - 37\lambda^2 + 22) \cosh\left(\frac{3x}{2}\right) + 24 \cosh\left(\frac{5x}{2}\right) \right) \\ & - \frac{1}{64} \operatorname{sech}^7\left(\frac{x}{2}\right) \left( -204\lambda^2 \sinh\left(\frac{x}{2}\right) + 222\lambda^2 \sinh\left(\frac{3x}{2}\right) \right. \\ & \left. + 206 \sinh\left(\frac{x}{2}\right) - 129 \sinh\left(\frac{3x}{2}\right) \right) - \frac{1}{64} \operatorname{sech}^7\left(\frac{x}{2}\right) \\ & \left( -90\lambda^4 \sinh\left(\frac{3x}{2}\right) + 18\lambda^4 \sinh\left(\frac{5x}{2}\right) - 42\lambda^2 \sinh\left(\frac{5x}{2}\right) \right. \\ & \left. + 25 \sinh\left(\frac{5x}{2}\right) \right), \end{aligned} \tag{63}$$

$$\begin{aligned} w_2(x, t) = & \frac{1}{2} + \frac{1}{2} \tanh\left(\frac{x}{2}\right) + \frac{1}{8} \operatorname{sech}^4\left(\frac{x}{2}\right) (3(\lambda^2 - 1) \sinh(x) \\ & + (3\lambda^2 - 4) \cosh(x) - 1) \frac{t^\alpha}{\alpha} - \frac{1}{64} \operatorname{sech}^7\left(\frac{x}{2}\right) \\ & \left( 18\lambda^4 \cosh\left(\frac{5x}{2}\right) - 42\lambda^2 \cosh\left(\frac{5x}{2}\right) \right. \\ & \left. - 24(\lambda^2 - 1) \cosh\left(\frac{x}{2}\right) \right) - \frac{1}{64} \operatorname{sech}^7\left(\frac{x}{2}\right) \\ & \left( -6(15\lambda^4 - 37\lambda^2 + 22) \cosh\left(\frac{3x}{2}\right) + 24 \cosh\left(\frac{5x}{2}\right) \right) \\ & - \frac{1}{64} \operatorname{sech}^7\left(\frac{x}{2}\right) \left( -204\lambda^2 \sinh\left(\frac{x}{2}\right) + 222\lambda^2 \sinh\left(\frac{3x}{2}\right) \right. \\ & \left. + 206 \sinh\left(\frac{x}{2}\right) - 129 \sinh\left(\frac{3x}{2}\right) \right) - \frac{1}{64} \operatorname{sech}^7\left(\frac{x}{2}\right) \\ & \left( -90\lambda^4 \sinh\left(\frac{3x}{2}\right) + 18\lambda^4 \sinh\left(\frac{5x}{2}\right) - 42\lambda^2 \sinh\left(\frac{5x}{2}\right) \right. \\ & \left. + 25 \sinh\left(\frac{5x}{2}\right) \right) \frac{t^{2\alpha}}{2\alpha^2}. \end{aligned} \tag{64}$$

Similarly, through this process, we obtain

$$\begin{aligned}
 w_n(x,t) = & \frac{1}{2} + \frac{1}{2} \tanh\left(\frac{x}{2}\right) + \frac{1}{8} \operatorname{sech}^4\left(\frac{x}{2}\right) (3(\lambda^2 - 1) \sinh(x) \\
 & + (3\lambda^2 - 4) \cosh(x) - 1) \frac{t^\alpha}{\alpha} - \frac{1}{64} \operatorname{sech}^7\left(\frac{x}{2}\right) \\
 & \left(18\lambda^4 \cosh\left(\frac{5x}{2}\right) - 42\lambda^2 \cosh\left(\frac{5x}{2}\right) - 24(\lambda^2 - 1) \cosh\left(\frac{x}{2}\right)\right) \\
 & - \frac{1}{64} \operatorname{sech}^7\left(\frac{x}{2}\right) \left(-6(15\lambda^4 - 37\lambda^2 + 22) \cosh\left(\frac{3x}{2}\right)\right. \\
 & \left.+ 24 \cosh\left(\frac{5x}{2}\right)\right) - \frac{1}{64} \operatorname{sech}^7\left(\frac{x}{2}\right) \left(-204\lambda^2 \sinh\left(\frac{x}{2}\right)\right) \\
 & + 222\lambda^2 \sinh\left(\frac{3x}{2}\right) + 206 \sinh\left(\frac{x}{2}\right) \frac{t^{2\alpha}}{2\alpha^2} + \dots
 \end{aligned} \tag{65}$$

If  $\alpha = 1$ , we obtain the exact solution

$$w(x,t) = \frac{1}{2} \tanh\left(\frac{x-t}{2}\right) + \frac{1}{2}. \tag{66}$$

### 3.2 Numerical simulation of the fractional-order nonlinear Cahn–Hilliard equation

Let us consider the equation

$$\frac{\partial^\alpha w}{\partial t} = \frac{\partial w}{\partial x} - 6w \left(\frac{\partial w}{\partial x}\right)^2 + (3w^2 - 1) \frac{\partial^2 w}{\partial x^2} - \frac{\partial^4 w}{\partial x^4}, \tag{67}$$

with an initial condition

$$w(x,0) = \tanh\left(\frac{\sqrt{2}x}{2}\right). \tag{68}$$

We use the fractional conformable residual power series algorithm for solving this equation. For this, the  $m$ -truncated term is

$$w_m = \zeta_0(x) + \sum_{i=1}^m \frac{t^{i\alpha} \zeta_i(x)}{i! \alpha^i}, \tag{69}$$

and the residual error function is

$$\mathcal{R}_s^m(x,t) = \frac{\partial^\alpha w_m}{\partial t} - \frac{\partial w_m}{\partial x} - 6w_m \left(\frac{\partial w_m}{\partial x}\right)^2 - 3w_m^2 - 1 \frac{\partial^2 w_m}{\partial x^2} + \frac{\partial^4 w_m}{\partial x^4}. \tag{70}$$

For  $m = 0$ ,

$$w_0(x,t) = \tanh\left(\frac{\sqrt{2}x}{2}\right).$$

For  $m = 1$ , the truncated term is

$$w_1(x,t) = \zeta_0(x) + \frac{\zeta_1(x)t^\alpha}{\alpha}, \tag{71}$$

$$\zeta_0(x) = w_0(x,t) = \tanh\left(\frac{\sqrt{2}x}{2}\right), \tag{72}$$

$$w_1(x,t) = \tanh\left(\frac{\sqrt{2}x}{2}\right) + \frac{\zeta_1(x)t^\alpha}{\alpha}. \tag{73}$$

Therefore, the first residual error function is

$$\mathcal{R}_s^1(x,t) = \frac{\partial^\alpha w_1}{\partial t} - w_1 - 6w_1 \left(\frac{\partial w_1}{\partial x}\right)^2 - (3w_1^2 - 1) \frac{\partial^2 w_1}{\partial x^2} + \frac{\partial^4 w_1}{\partial x^4}. \tag{74}$$

Substituting Eq. 71 into Eq. 74, we obtain

$$\begin{aligned}
 \mathcal{R}_s^1(x,t) = & \frac{\partial^\alpha}{\partial t} \left(\frac{\zeta_1(x)t^\alpha}{\alpha} + \zeta_0(x)\right) - \frac{\partial}{\partial x} \left(\zeta_0(x) + \frac{\zeta_1(x)t^\alpha}{\alpha}\right) \\
 & - 6 \left(\zeta_0(x) + \frac{\zeta_1(x)t^\alpha}{\alpha}\right) \left(\frac{\partial}{\partial x} \zeta_0 + \frac{\zeta_1 x t^\alpha}{\alpha}\right)^2 \\
 & - \left(3 \left(\zeta_0(x) + \frac{\zeta_1 x t^\alpha}{\alpha}\right)^2 - 1\right) \frac{\partial^2}{\partial x^2} \left(\frac{\zeta_1(x)t^\alpha}{\alpha} + \zeta_0(x)\right) \\
 & + \frac{\partial^4}{\partial x^4} \left(\zeta_0(x) + \frac{\zeta_1(x)t^\alpha}{\alpha}\right).
 \end{aligned} \tag{75}$$

Thus,  $R_s^1(x,t)$  at  $t = 0$ ,

$$-6\zeta_0(x)\zeta_0'(x)^2 - (3\zeta_0(x)^2 - 1)\zeta_0''(x) - \zeta_0(x) + \zeta_0^4(x) + \zeta_1(x) = 0, \tag{76}$$

$$\zeta_1(x) = \frac{\operatorname{sech}^2\left(\frac{x}{\sqrt{2}}\right)}{\sqrt{2}}. \tag{77}$$

Therefore, the first series solution  $w_1(x,t)$  is provided by

$$w_1(x,t) = \tanh\left(\frac{\sqrt{2}x}{2}\right) + \frac{\operatorname{sech}^2\left(\frac{x}{\sqrt{2}}\right)t^\alpha}{\sqrt{2}\alpha}. \tag{78}$$

For  $m = 2$ , the truncated term is

$$w_2(x,t) = \frac{\zeta_2(x)t^{2\alpha}}{2\alpha^2} + \frac{\zeta_1(x)t^\alpha}{\alpha} + \zeta_0(x), \tag{79}$$

$$w_2(x,t) = \tanh\left(\frac{\sqrt{2}x}{2}\right) + \frac{\operatorname{sech}^2\left(\frac{x}{\sqrt{2}}\right)t^\alpha}{\sqrt{2}\alpha} + \frac{\zeta_2(x)t^{2\alpha}}{2\alpha^2}. \tag{80}$$

Substituting Eq. 79 into Eq. 80, the second residual error function is

$$\begin{aligned}
 \mathcal{R}_s^2(x,t) = & \frac{\partial^\alpha}{\partial t} \left(\frac{t^{2\alpha} \zeta_2(x)}{2\alpha^2} + \frac{t^\alpha \zeta_1(x)}{\alpha} + \zeta_0(x)\right) \\
 & - \frac{\partial}{\partial x} \left(\frac{t^{2\alpha} \zeta_2(x)}{2\alpha^2} + \frac{t^\alpha \zeta_1(x)}{\alpha} + \zeta_0(x)\right) \\
 & - 6 \left(\frac{t^{2\alpha} \zeta_2(x)}{2\alpha^2} + \frac{\zeta_1 x t^\alpha}{\alpha} + \zeta_0(x)\right) \\
 & \frac{\partial}{\partial x} \left(\frac{t^{2\alpha} \zeta_2(x)}{2\alpha^2} + \frac{t^\alpha \zeta_1(x)}{\alpha} + \zeta_0(x)\right)^2 \\
 & - \left(3 \left(\frac{t^{2\alpha} \zeta_2(x)}{2\alpha^2} + \frac{\zeta_1 x t^\alpha}{\alpha} + \zeta_0(x)\right)^2 - 1\right) \\
 & \frac{\partial^2}{\partial x^2} \left(\frac{t^{2\alpha} \zeta_2(x)}{2\alpha^2} + \frac{t^\alpha \zeta_1(x)}{\alpha} + \zeta_0(x)\right) \\
 & + \frac{\partial^4}{\partial x^4} \left(\frac{t^{2\alpha} \zeta_2(x)}{2\alpha^2} + \frac{\zeta_1 x t^\alpha}{\alpha} + \zeta_0(x)\right),
 \end{aligned} \tag{81}$$



$$\begin{aligned} \mathcal{R}_s^2(x, t) = & \left( \frac{t^\alpha \zeta_2(x)}{\alpha} + \zeta_1(x) \right) - \left( \frac{t^{2\alpha} \zeta_2'(x)}{2\alpha^2} + \frac{t^\alpha \zeta_1'(x)}{\alpha} + \zeta_0'(x) \right) \\ & - 6 \left( \frac{t^{2\alpha} \zeta_2(x)}{2\alpha^2} + \frac{t^\alpha \zeta_1(x)}{\alpha} + \zeta_0(x) \right) \\ & \left( \frac{t^{2\alpha} \zeta_2'(x)}{2\alpha^2} + \frac{t^\alpha \zeta_1'(x)}{\alpha} + \zeta_0'(x) \right)^2 \\ & - \left( 3 \left( \frac{t^{2\alpha} \zeta_2(x)}{2\alpha^2} + \frac{t^\alpha \zeta_1(x)}{\alpha} + \zeta_0(x) \right)^2 - 1 \right) \\ & \left( \frac{t^{2\alpha} \zeta_2''(x)}{2\alpha^2} + \frac{t^\alpha \zeta_1''(x)}{\alpha} + \zeta_0''(x) \right) \\ & + \left( \frac{t^{2\alpha} \zeta_2^4(x)}{2\alpha^2} + \frac{t^\alpha \zeta_1^4(x)}{\alpha} + \zeta_0^4(x) \right). \end{aligned} \tag{82}$$

Then,  $d^\alpha/dt$  is applied on both sides of Eq. 82 and thus at  $t = 0$ , we obtain

$$\begin{aligned} \zeta_2(x) = & 12\zeta_0(x)\zeta_0'(x)\zeta_1'(x) + 6\zeta_1(x)\zeta_0'(x)^2 + 3\zeta_0(x)^2\zeta_1''(x) \\ & + 6\zeta_1(x)\zeta_0(x)\zeta_0''(x) - \zeta_1''(x) + \zeta_1(x) - \zeta_1^4(x), \end{aligned} \tag{83}$$

$$\zeta_2(x) = \tanh\left(\frac{x}{\sqrt{2}}\right) \left( -\operatorname{sech}^2\left(\frac{x}{\sqrt{2}}\right) \right), \tag{84}$$

$$\begin{aligned} w_2(x, t) = & \frac{t^{2\alpha} \tanh\left(\frac{x}{\sqrt{2}}\right) \left( -\operatorname{sech}^2\left(\frac{x}{\sqrt{2}}\right) \right)}{2\alpha^2} + \frac{t^\alpha \operatorname{sech}^2\left(\frac{x}{\sqrt{2}}\right)}{\sqrt{2}\alpha} \\ & + \tanh\left(\frac{\sqrt{2}x}{2}\right). \end{aligned} \tag{85}$$

Similarly, through this process, we obtain

$$\begin{aligned} w_3(x, t) = & \frac{1}{16} \operatorname{sech}^6\left(\frac{x}{\sqrt{2}}\right) \left( \tanh\left(\frac{x}{\sqrt{2}}\right) (\sqrt{2} \sinh(2\sqrt{2}x)) \right) \\ & \frac{1}{16} \operatorname{sech}^6\left(\frac{x}{\sqrt{2}}\right) \left( (-224 \cosh(\sqrt{2}x) + 4 \cosh(2\sqrt{2}x) + 492) - 4\sqrt{2} \right), \end{aligned} \tag{86}$$

$$\begin{aligned} w_n(x, t) = & \frac{t^{2\alpha} \tanh\left(\frac{x}{\sqrt{2}}\right) \left( -\operatorname{sech}^2\left(\frac{x}{\sqrt{2}}\right) \right)}{2\alpha^2} + \frac{t^\alpha \operatorname{sech}^2\left(\frac{x}{\sqrt{2}}\right)}{\sqrt{2}\alpha} \\ & + \tanh\left(\frac{\sqrt{2}x}{2}\right) + \frac{1}{16} \operatorname{sech}^6\left(\frac{x}{\sqrt{2}}\right) \\ & \left( \tanh\left(\frac{x}{\sqrt{2}}\right) (\sqrt{2} \sinh(2\sqrt{2}x) - 224 \cosh(\sqrt{2}x) \right. \\ & \left. + 4 \cosh(2\sqrt{2}x) + 492) - 4\sqrt{2} \right) + \dots \end{aligned} \tag{87}$$

If  $\alpha = 1$ , we obtain the exact solution

$$w(x, t) = \tanh\left(\frac{\sqrt{2}(x+t)}{2}\right). \tag{88}$$

### 4 Stability analysis

In this section, we examine the stability property [35] for Eqs 1, 2. Understanding the stability of an equilibrium solution may be gained by linearizing the FNLPE around it. In order to investigate

the rise or decay of minor perturbations, eigenvalue analysis is performed on the linearized equation, which has fractional derivatives. By solving the characteristic equation linked to the linearized system, the eigenvalues may be found. The equilibrium is stable if all of the eigenvalues have negative real portions; otherwise, it is unstable. Nevertheless, it is crucial to keep in mind that the fractional character of the derivatives makes the eigenvalue analysis more complicated. A Hamiltonian system is used to investigate the stability feature of the nonlinear fractional equations. The Hamiltonian system’s momentum is represented using the following formula:

$$H = 1/2 \int_{-k}^k w^2(x), dx. \tag{89}$$

Consequently, the condition for the stability of solutions is as follows:

$$\frac{\partial H}{\partial v} > 0. \tag{90}$$

For example, we check the stability property for Eq. 24, and we obtain

$$H = \frac{2\vartheta^4 \left( \frac{\sigma(-(\nu-10)) + \frac{4}{\sigma(\nu-10)-2} - 4 \log(10\sigma + \sigma(-\nu)+2)}{\sigma^3} - \frac{\sigma(-(\nu+10)) + \frac{4}{\sigma(\nu+10)-2} - 4 \log(2-\sigma(\nu+10))}{\sigma^3} \right)}{\lambda^2}. \tag{91}$$

Therefore,

$$\frac{\partial H}{\partial \nu} \Big|_{\nu=2} = 1.6 > 0. \tag{92}$$

So, this solution is stable on the interval  $x \in [-10, 10]$ . Similarly, we can check the stability of other obtained solutions with our novel technique.

### 5 Results and discussion

The MAEM and methods for fractional conformable residual power series are designed particularly to handle fractional equations. They take into account the special characteristics and behaviors related to fractional calculus and are designed to operate with fractional derivatives. These techniques offer specialized tools that are ideally suited for studying FNLPEs with fractional-order derivatives. When compared to other numerical techniques, the MAEM and fractional conformable residual power series algorithms can provide computational efficiency. They frequently require shortening series expansions or solving auxiliary equations, which can lower the complexity and expense of computing. This benefit may be especially important when handling complex or computationally difficult FNLPEs. Table 1 presents a comparison of the absolute error  $|w - w_2|$  of both equations. These results clearly demonstrate the accuracy and effectiveness of the numerical technique. The results of the MAEM include the periodic and singular solutions. Utilizing 3D surface plots, 2D contour plots, density graphs, and 2D line graphs, the graphical simulation of a few retrieved solutions is discussed. The graphs are created for appropriate values of the arbitrary parameters  $\alpha, \lambda$ , and  $\vartheta$ .

Figure 1 shows the 3D, 2D, and counterplot graphs at  $\alpha = 1$ ,  $\lambda = 1$ ,  $\vartheta = -1$ , and  $t = 5$  of  $v_{1,1}(x, t)$ . Similarly, Figure 2 shows the 3D, 2D, and counterplot graphs at  $\alpha = 1$ ,  $\lambda = 1$ ,  $\vartheta = 1$ , and  $t = 10$ , which is a periodic solitary wave of  $v_{1,3}(x, t)$ . Figure 3 shows the 3D, 2D, and counterplot graphs at  $\alpha = 1$ ,  $\lambda = 1$ ,  $\vartheta = -1$ , and  $t = 0.5, 1, 1.5$  of  $v_{1,5}(x, t)$ . Similarly, Figure 4 shows the 3D, 2D, and counterplot graphs at  $\alpha = 1$  and  $t = 5$  of  $v_{1,7}(x, t)$ . Figure 5 shows the 3D, 2D, and counterplot graphs at  $\theta = 1$  and  $\vartheta = 0.1$  of  $v_{2,2}(x, t)$ . Similarly, Figure 6 shows the 3D, 2D, and counterplot graphs at  $\theta = 1$  and  $\vartheta = 0.1$ , which is periodic solitary wave of  $v_{2,4}(x, t)$ . Figure 7 shows the 3D, 2D, and counterplot graphs at  $\alpha = 1$ , which is a singular soliton solution of  $v_{2,5}(x, t)$ . Figure 8 shows the 3D, 2D, and counterplot graphs at  $\theta = 1$  and  $\vartheta = 0.1$ , which is periodic solitary wave of  $v_{2,4}(x, t)$ . Figure 9 shows the 3D, 2D, and counterplot graphs at  $\alpha = 1$ , which is a singular soliton solution of  $v_{2,5}(x, t)$ . Figure 10 shows the 3D, 2D, and counterplot graphs at  $\theta = 1$  and  $\vartheta = 0.1$ , which is a periodic solitary wave of  $v_{2,4}(x, t)$ . Figure 11 shows the comparison of error terms between numerical and analytical techniques. Figure 12 shows the comparison between numerical and analytical techniques. Figure 13 shows the stability analysis of governing equations. Fundamental mathematical techniques used to describe and examine real-world occurrences in science and engineering include trigonometric, hyperbolic, and rational functions. In order to represent oscillatory motion and periodic phenomena like waves and tides, trigonometric functions like sine and cosine are used. Heat conduction, population expansion, and fluid dynamics are the three areas where hyperbolic functions, such as hyperbolic sine and cosine, are used to depict exponential growth and decay. Rational functions, which are polynomial ratios, have asymptotes, holes, and other graph characteristics that make them useful for simulating complex systems in financial analysis, control systems, population dynamics, and circuit design.

## 6 Conclusion

The nonlinear fractional Cahn–Hilliard and Gardner equations have been addressed in this paper using a unique methodology. This analytical technique is useful for creating partial differential equations and discovering approximate solutions under the right initial circumstances. The effectiveness of the suggested method is also shown by the precise results obtained utilizing MAEM with a smaller number of series terms. The application of this method to two different physical models demonstrates its accuracy and efficiency in handling fractional nonlinear equations, leading to stunning and complicated graphics. Additionally, the approximation series' quick convergence is noted. We can see how the graphs change as a result of changing parameter values. When the calculations and simulations performed in

Mathematica 11 were compared to previous numerical findings, it became clear that this numerical method is capable of handling difficult fractional equations in higher dimensions. The analytical approach used here is also notable for being straightforward, reliable, and succinct when solving nonlinear partial differential equations. The overall findings of the study emphasize the importance of this strategy in improving our knowledge and management of such difficult equations.

## Data availability statement

The original contributions presented in the study are included in the article/Supplementary Material; further inquiries can be directed to the corresponding author.

## Author contributions

AA: writing, conceptualization, formal analysis, supervision, and review and editing. AN: review implementation and editing. MN: formal analysis and review and editing. MJB: formal analysis and review and editing. AF: formal analysis and writing the original draft. AFA: formal analysis and review and editing. RH: formal analysis and review and editing. All authors contributed to the article and approved the submitted version.

## Acknowledgments

The authors extend their appreciation to the Researchers Supporting Project (No. RSP2023R218), King Saud University, Riyadh, Saudi Arabia.

## Conflict of interest

The authors declare that the research was conducted in the absence of any commercial or financial relationships that could be construed as a potential conflict of interest.

## Publisher's note

All claims expressed in this article are solely those of the authors and do not necessarily represent those of their affiliated organizations, or those of the publisher, the editors, and the reviewers. Any product that may be evaluated in this article, or claim that may be made by its manufacturer, is not guaranteed or endorsed by the publisher.

## References

1. Ali A, Ahmad J, Javed S. Solitary wave solutions for the originating waves that propagate of the fractional Wazwaz–Benjamin–Bona–Mahony system. *Alexandria Eng J* (2023) 69:121–33. doi:10.1016/j.aej.2023.01.063
2. Ali A, Ahmad J, Javed S. Exploring the dynamic nature of soliton solutions to the fractional coupled nonlinear Schrödinger model with their sensitivity analysis. *Opt Quan Elect* (2023) 55(9):810. doi:10.1007/s11082-023-05033-y

3. Wang KJ. Traveling wave solutions of the Gardner equation in dusty plasmas. *Results Phys* (2022) 33:105207. doi:10.1016/j.rinp.2022.105207
4. Kudryashov NA. Optical solitons of the model with generalized anti-cubic nonlinearity. *Optik* (2022) 257:168746. doi:10.1016/j.ijleo.2022.168746
5. Wang KJ. Variational principle and diverse wave structures of the modified Benjamin-Bona-Mahony equation arising in the optical illusions field. *Axioms* (2022) 11(9):445. doi:10.3390/axioms11090445
6. Ali A, Ahmad J, Javed S, Rehman SU. Analysis of chaotic structures, bifurcation and soliton solutions to fractional Boussinesq model. *Physica Scripta* (2023) 98:075217. doi:10.1088/1402-4896/acdcee
7. Islam SR, Arafat SY, Wang H. Abundant closed-form wave solutions to the simplified modified Camassa-Holm equation. *J Ocean Eng Sci* (2022) 8:238–45. doi:10.1016/j.joes.2022.01.012
8. Shakeel M, El-Zahar ER, Shah NA, Chung JD. Generalized exp-function method to find closed form solutions of nonlinear dispersive modified benjamin-bona-mahony equation defined by seismic sea waves. *Mathematics* (2022) 10(7):1026. doi:10.3390/math10071026
9. Joseph SP. Exact traveling wave doubly periodic solutions for generalized double sine-gordon equation. *Int J Appl Comput Math* (2022) 8(1):42–19. doi:10.1007/s40819-021-01236-7
10. Athron P, Fowle A, Lu CT, Wu L, Wu Y, Zhu B. *The W boson mass and muon g - 2: Hadronic uncertainties or new physics?* (2022). arXiv preprint arXiv:2204.03996.
11. Seidel A. *Integral approach for hybrid manufacturing of large structural titanium space components* (2022).
12. Saifullah S, Ahmad S, Alyami MA, Inc M. Analysis of interaction of lump solutions with kink-soliton solutions of the generalized perturbed KdV equation using Hirota-bilinear approach. *Phys Lett A* (2022) 454:128503. doi:10.1016/j.physleta.2022.128503
13. Liu SZ, Wang J, Zhang DJ. The fokas-lenells equations: bilinear approach. *Stud Appl Math* (2022) 148(2):651–88. doi:10.1111/sapm.12454
14. Khater MM. Prorogation of waves in shallow water through unidirectional Dullin-Gottwald-Holm model; computational simulations. *Int J Mod Phys B* (2022) 37:2350071. doi:10.1142/s0217979223500716
15. Muniyappan A, Sahasraari LN, Anitha S, Ilakiya S, Biswas A, Yıldırım Y, et al. Family of optical solitons for perturbed Fokas-Lenells equation. *Optik* (2022) 249:168224. doi:10.1016/j.ijleo.2021.168224
16. He XJ, Lü X. M-lump solution, soliton solution and rational solution to a (3+1)-dimensional nonlinear model. *Mathematics Comput Simulation* (2022) 197:327–40. doi:10.1016/j.matcom.2022.02.014
17. Zhang T, Li M, Chen J, Wang Y, Miao L, Lu Y, et al. Multi-component ZnO alloys: bandgap engineering, hetero-structures, and optoelectronic devices. *Mater Sci Eng R: Rep* (2022) 147:100661. doi:10.1016/j.mser.2021.100661
18. Min R, Hu X, Pereira L, Soares MS, Silva LC, Wang G, et al. Polymer optical fiber for monitoring human physiological and body function: A comprehensive review on mechanisms, materials, and applications. *Opt Laser Technol* (2022) 147:107626. doi:10.1016/j.optlastec.2021.107626
19. Lechelon M, Meriguet Y, Gori M, Ruffenach S, Nardecchia I, Floriani E, et al. Experimental evidence for long-distance electrodynamic intermolecular forces. *Sci Adv* (2022) 8(7):eabl5855. doi:10.1126/sciadv.abl5855
20. Tarla S, Ali KK, Yilmazer R, Yusuf A. Investigation of the dynamical behavior of the Hirota-Maccari system in single-mode fibers. *Opt Quan Elect* (2022) 54(10):613–2. doi:10.1007/s11082-022-04021-y
21. Ahmad J, Rizwanullah M, Suthar T, Albarqi HA, Ahmad MZ, Vuddanda PR, et al. Receptor-targeted surface-engineered nanomaterials for breast cancer imaging and theranostic applications. *The Eur Phys J D* (2022) 76(1):1–44. doi:10.1615/CritRevTherDrugCarrierSyst.2022040686
22. Dubey S, Chakraverty S. Application of modified extended tanh method in solving fractional order coupled wave equations. *Math Comput Simulation* (2022) 198:509–20. doi:10.1016/j.matcom.2022.03.007
23. Siddique I, Mehdi KB, Jarad F, Elbrolosy ME, Elmandouh AA. Novel precise solutions and bifurcation of traveling wave solutions for the nonlinear fractional (3+1)-dimensional WBBM equation. *Int J Mod Phys B* (2022) 37:2350011. doi:10.1142/s021797922350011x
24. Jiang Y, Wang F, Salama SA, Botmart T, Khater MM. Computational investigation on a nonlinear dispersion model with the weak non-local nonlinearity in quantum mechanics. *Results Phys* (2022) 38:105583. doi:10.1016/j.rinp.2022.105583
25. Bilal M, Rehman SU, Ahmad J. The study of new optical soliton solutions to the time-space fractional nonlinear dynamical model with novel mechanisms. *J Ocean Eng Sci* (2022). doi:10.1016/j.joes.2022.05.027
26. Fu Z, Liu S, Liu S. New kinds of solutions to Gardner equation. *Chaos, Solitons & Fractals* (2004) 20(2):301–9. doi:10.1016/s0960-0779(03)00383-7
27. Chen W, Sun H, Li XC. *Fractional derivative modelling in mechanics and engineering*. Springer (2022).
28. Abouelregal AE, Fahmy MA. Generalized Moore-Gibson-Thompson thermoelastic fractional derivative model without singular kernels for an infinite orthotropic thermoelastic body with temperature-dependent properties. *ZAMM-Journal Appl Math Mechanics/Zeitschrift für Angew Mathematik Mechanik* (2022) 102:e202100533. doi:10.1002/zamm.202100533
29. Zhu Y, Tang T, Zhao S, Joralmon D, Poit Z, Ahire B, et al. Recent advancements and applications in 3D printing of functional optics. *Additive Manufacturing* (2022) 52:102682. doi:10.1016/j.addma.2022.102682
30. Li Q, Shan W, Wang P, Cui H. Breather, lump and N-soliton wave solutions of the (2+1)-dimensional coupled nonlinear partial differential equation with variable coefficients. *Commun Nonlinear Sci Numer Simulation* (2022) 106:106098. doi:10.1016/j.cnsns.2021.106098
31. Prakasha DG, Veeresha P, Baskonus HM. Two novel computational techniques for fractional Gardner and Cahn-Hilliard equations. *Comput Math Methods* (2019) 1(2):e1021. doi:10.1002/cmm4.1021
32. Aniq A, Ahmad J. Soliton solution of fractional Sharma-Tasso-Olevers equation via an efficient (G'/G)-expansion method. *Ain Shams Eng J* (2022) 13(1):101528. doi:10.1016/j.asej.2021.06.014
33. Khater M, Lu D, Attia RA. Dispersive long wave of nonlinear fractional Wu-Zhang system via a modified auxiliary equation method. *AIP Adv* (2019) 9(2). doi:10.1063/1.5087647
34. Scarmozzino R, Gopinath A, Pregla R, Helfert S. Numerical techniques for modeling guided-wave photonic devices. *IEEE J Selected Top Quan Elect* (2000) 6(1):150–62. doi:10.1109/2944.826883
35. Ali A, Ahmad J, Javed S. Stability analysis and novel complex solutions to the malaria model utilising conformable derivatives. *The Eur Phys J Plus* (2023) 138(3):259–17. doi:10.1140/epjp/s13360-023-03851-3